

---

# Bayesian Persuasion with a Risk-Conscious Receiver

---

Yujing Chen

School of Mathematical Sciences, Peking University  
yujingchen@stu.pku.edu.cn

## Abstract

We study Bayesian persuasion when the receiver evaluates actions by reward-side Conditional Value-at-Risk (CVaR) rather than expected utility. CVaR preferences break the standard action-based direct-recommendation reduction: merging signals that recommend the same action can change the receiver’s tail-risk ranking and destroy incentive compatibility. We show that this failure does not imply intractability in the explicit finite-state model. Each CVaR action value is max-affine in the posterior, and refining recommendations by the active affine piece yields an active-facet revelation principle and an exact polynomial-size linear program. We further identify a representation boundary: listed polyhedral risks remain tractable by the same LP, whereas succinctly represented facet families make exact persuasion NP-hard. Finally, we give a finite-precision approximation scheme for risk preferences determined by finitely many stable posterior statistics.

## 1 Introduction

In many strategic communication settings, a sender influences a receiver by selectively revealing information about an uncertain state of the world. Bayesian persuasion, introduced by Kamenica and Gentzkow [2011], gives a clean formal model for this problem and has found applications in advertising, security, regulation, and resource allocation [Badanidiyuru et al., 2018, Rabinovich et al., 2015, Yang et al., 2013]. The classical theory usually assumes that the receiver is risk-neutral, so her payoff from an action is linear in the posterior belief. This linearity is mathematically powerful: it supports the revelation principle and leads to tractable linear-programming formulations.

Many decision environments violate this premise. A regulator evaluating a model release, a platform deciding whether to surface an automated recommendation, or an operator deciding whether to trust an alert may care less about average performance than about rare but severe failures. In such settings, the receiver may reject an action that looks favorable in expectation if a small posterior tail contains unacceptable downside risk. The information-design problem is then not only to persuade an expected-utility receiver, but to communicate in a way that remains persuasive under tail-risk evaluation.

We capture this form of caution through Conditional Value-at-Risk (CVaR), a standard risk measure that focuses on the worst tail of an outcome distribution [Artzner et al., 1999, Rockafellar and Uryasev, 2000, 2002, Acerbi and Tasche, 2002, Jorion, 2006, Filippi et al., 2020]. Under CVaR preferences, the receiver’s utility is nonlinear in posterior beliefs. As a result, merging two signals that separately induce the same action can destroy incentive compatibility, so direct recommendation schemes are no longer without loss. Recent work has developed geometric insight for risk-conscious receivers [Anunrojwong et al., 2024]; this paper gives a computational account of the CVaR case.

**Our contributions.** The paper studies how tail-risk preferences alter the reduced form and computational structure of Bayesian persuasion. The first observation is that CVaR, and more generally nonlinear risk preferences, can invalidate the usual action-based revelation argument. Under expected utility, the receiver’s incentive constraints are linear in the posterior, so signals that induce the same

action can be merged. Under CVaR, merging changes the distribution of outcomes under the posterior and may change the relevant lower tail. An action that is optimal at two posteriors need not remain optimal at their convex combination.

The main positive result is an active-facet replacement for direct revelation. In a finite state space, the CVaR value of each action is max-affine in the posterior. A signal can therefore be indexed by an action  $a$  together with an active affine piece  $\ell$  supporting the receiver’s CVaR value. Conditional on this action-facet pair, incentive compatibility is described by linear inequalities. This gives an active-facet revelation principle and an exact linear program with polynomially many variables and constraints in the explicit finite-state model.

The same argument also clarifies the role of representation. CVaR is one instance of an explicitly listed polyhedral risk preference,  $\rho(\mu, a) = \max_{\ell \in \mathcal{L}_a} \langle c_{a,\ell}, \mu \rangle$ . Whenever the affine pieces are part of the input, the active-facet LP remains polynomial in the listed representation. By contrast, if the affine pieces are specified only implicitly by a succinct combinatorial family, the representation can hide an NP-hard search problem. We prove such a hardness result for succinct polyhedral risk preferences with an explicit finite state space and two receiver actions.

The approximation results address this representation gap. They are not needed to solve the tabular CVaR problem, but they give a finite-precision method for settings in which the exact facet description is unavailable or too large. Under a finite-statistic access condition, where the receiver’s risk value depends Lipschitz-continuously on finitely many posterior statistics and the induced statistic cells can be enforced, a discretized state-contingent LP gives uniform  $\epsilon$ -incentive compatibility. A positive margin condition converts this approximate guarantee into strict incentive compatibility, and a local active-facet refinement shows how the grid complexity can depend on the number of facets that are active near the relevant posterior region rather than on the global facet count.

## 1.1 Related Work

We give a short overview here and defer a fuller discussion to Appendix B. Bayesian persuasion was introduced by Kamenica and Gentzkow [2011]; see Bergemann and Morris [2019] for a survey. Classical tractability relies on expected-utility linearity, which supports concavification and direct recommendations. We ask what remains when the receiver evaluates actions by tail risk.

The closest conceptual predecessor is work on risk-conscious receivers [Anunrojwong et al., 2024]. We focus on CVaR and show that its finite max-affine representation yields an active-facet revelation principle and an exact LP in the explicit finite-state model. This connects to algorithmic persuasion, where LP tractability is well understood under expected utility [Xu et al., 2015, Dughmi and Xu, 2021]. The explicit-versus-succinct distinction used here follows a standard representation view in complexity theory: compact encodings can change the complexity of graph and combinatorial problems [Galperin and Wigderson, 1983, Papadimitriou and Yannakakis, 1986, Wagner, 1986]. In our setting, listed polyhedral risks remain tractable, while succinctly represented facet families can be hard.

The finite-precision part uses the sampling intuition behind sparse approximations in games [Althöfer, 1994, Lipton et al., 2003], but the approximated objects are posterior statistics determining the receiver’s risk value rather than mixed strategies or payoff vectors.

## 2 The General Risk-Conscious Persuasion Model

We first describe a persuasion model in which the receiver’s preference over actions may be nonlinear in posterior beliefs. This general formulation keeps the role of the risk functional separate from the information structure; CVaR is introduced in the next section.

### 2.1 The Environment and Information Structure

We consider a game with a single Sender ( $S$ ) and a single Receiver ( $R$ ). The uncertainty is a state  $\omega$  drawn from a finite state space  $\Omega = \{\omega_1, \dots, \omega_m\}$ . The Sender and Receiver share a common prior  $\mu_0 \in \text{int}(\Delta(\Omega))$ , where  $\Delta(\Omega)$  is the  $(m - 1)$ -dimensional probability simplex over  $\Omega$ . The Receiver chooses from a finite action set  $\mathcal{A} = \{a_1, \dots, a_n\}$ . Throughout the paper, we write  $n = |\mathcal{A}|$ .

The Sender possesses an informational advantage, observing the realization of the true state  $\omega$ . To influence the Receiver's action, the Sender commits to a *signaling scheme* (or information structure)  $\pi$ .

**Definition 1** (Signaling Scheme). *A signaling scheme is a tuple  $(\mathcal{S}, \pi)$ , where  $\mathcal{S}$  is a finite space of signal realizations, and  $\pi : \Omega \rightarrow \Delta(\mathcal{S})$  is a mapping from states to distributions over signals. We denote  $\pi(s|\omega)$  as the probability of sending signal  $s \in \mathcal{S}$  conditional on the realized state being  $\omega$ .*

Upon observing a signal  $s \in \mathcal{S}$ , the Receiver updates her belief about the state of the world using Bayes' rule. The posterior belief  $\mu_s \in \Delta(\Omega)$  is given by:

$$\mu_s(\omega) = \frac{\pi(s|\omega)\mu_0(\omega)}{\sum_{\omega' \in \Omega} \pi(s|\omega')\mu_0(\omega')}, \quad \forall \omega \in \Omega. \quad (1)$$

The unconditional probability of observing signal  $s$  is  $\mathbb{P}(s) = \sum_{\omega'} \pi(s|\omega')\mu_0(\omega')$ . Thus a signaling scheme induces a distribution of posterior beliefs  $\tau \in \Delta(\Delta(\Omega))$ . Bayesian updating imposes the Bayes-plausibility condition that the mean posterior equals the prior:

$$\sum_{s \in \mathcal{S}} \mathbb{P}(s)\mu_s = \mu_0. \quad (2)$$

## 2.2 Generalized Risk Preferences

In the canonical Bayesian persuasion model, the Receiver is assumed to be risk-neutral, maximizing an expected utility  $\mathbb{E}_{\mu_s}[u^R(\omega, a)]$  which is strictly linear in the posterior belief  $\mu_s$ .

In the generalized model, the Receiver evaluates actions through a risk functional  $\rho : \Delta(\Omega) \times \mathcal{A} \rightarrow \mathbb{R}$ . Given posterior  $\mu_s$ , the Receiver chooses

$$a^*(s) \in \operatorname{argmax}_{a \in \mathcal{A}} \rho(\mu_s, a). \quad (3)$$

Throughout, incentive compatibility is understood in the weak sense: a recommended action must belong to the receiver's best-response set. When the sender's value is evaluated at a posterior with multiple receiver best responses, we use sender-favorable tie-breaking.

The functional  $\rho$  may depend nonlinearly on  $\mu_s$ , allowing the model to represent preferences such as tail-risk sensitivity or ambiguity aversion. The Sender is risk-neutral with utility  $v : \Omega \times \mathcal{A} \rightarrow \mathbb{R}$  and solves the following bilevel problem:

$$\begin{aligned} \max_{\pi: \Omega \rightarrow \Delta(\mathcal{S})} \quad & \sum_{\omega \in \Omega} \sum_{s \in \mathcal{S}} \mu_0(\omega) \pi(s|\omega) v(\omega, a^*(s)) \\ \text{s.t.} \quad & a^*(s) \in \operatorname{argmax}_{a \in \mathcal{A}} \rho(\mu_s, a) \quad \forall s \in \mathcal{S} \\ & \sum_{s \in \mathcal{S}} \pi(s|\omega) = 1 \quad \forall \omega \in \Omega \\ & \pi(s|\omega) \geq 0 \quad \forall s \in \mathcal{S}, \omega \in \Omega \end{aligned} \quad (4)$$

## 2.3 Failure of Action-Based Revelation

The nonlinear dependence of  $\rho(\mu, a)$  on posterior beliefs changes the standard reduced form of Bayesian persuasion. Under expected utility, the receiver's payoff from each action is linear in  $\mu$ . If two signals both make the same action optimal, their merger preserves optimality, and the sender can restrict attention to direct recommendations indexed by actions.

This argument fails for general risk functionals. The set  $\{\mu \in \Delta(\Omega) : a \in \operatorname{argmax}_{a'} \rho(\mu, a')\}$  need not be convex. Hence two posteriors that both induce action  $a$  may have a convex combination at which another action is preferred. Merging signals that recommend the same action can therefore destroy incentive compatibility.

The failure of action-based revelation does not by itself imply computational hardness. It means that a different reduced form is needed. For arbitrary nonlinear risk preferences, such a reduced form may not be available. The next section shows that CVaR has enough additional structure to recover tractability: its value is max-affine in the posterior, and signals can be refined by the active affine facet supporting the recommended action.

For completeness, Appendix E records a standard finite-support bound for arbitrary risk preferences. This bound is a geometric background result and is not used in the active-facet LP construction.

### 3 Tractability and Optimization under CVaR

We now specialize the receiver's risk functional to Conditional Value-at-Risk (CVaR). The role of this specialization is structural. Although CVaR is nonlinear in posterior beliefs, it is polyhedral on every finite state space: for each action, the receiver's value is the maximum of finitely many affine functions. This max-affine structure is what makes an exact optimization result possible.

#### 3.1 CVaR-Conscious Preferences and Piecewise Linearity

For a given confidence level  $r \in (0, 1)$ , the Receiver evaluates the CVaR of the utility  $u(\omega, a)$ , which captures the expectation of the worst  $r$ -quantile outcomes. The risk functional is defined as:

$$\rho(\mu, a) := \text{CVaR}_r^\mu(u(\cdot, a)) = \sup_{b \in \mathbb{R}} \left( b - \frac{1}{r} \mathbb{E}_{\omega \sim \mu} [(b - u(\omega, a))^+] \right). \quad (5)$$

Although CVaR is nonlinear in beliefs, it has a simple finite-facet representation on a finite state space.

**Lemma 1** (Finite-Facet Representation of CVaR). *For any fixed action  $a \in \mathcal{A}$ , the function  $f_a(\mu) = \text{CVaR}_r^\mu(u(\cdot, a))$  is continuous, convex, and piecewise linear in  $\mu$ . More precisely, there exists a finite set  $\mathcal{L}_a$  with  $|\mathcal{L}_a| \leq |\Omega|$  and vectors  $c_{a,l} \in \mathbb{R}^{|\Omega|}$  such that*

$$f_a(\mu) = \max_{l \in \mathcal{L}_a} \langle c_{a,l}, \mu \rangle. \quad (6)$$

If  $|u(\omega, a)| \leq C_R$  for all  $(\omega, a)$ , then the coefficients may be chosen to satisfy

$$\|c_{a,l}\|_\infty \leq C_R \left( 1 + \frac{2}{r} \right). \quad (7)$$

Proof in Appendix G.

#### 3.2 Active-Facet Revelation and Exact Optimization

Lemma 1 shows that the receiver's CVaR value is nonlinear but finitely piecewise linear in posterior beliefs. This finite-facet structure gives the right replacement for the usual action-based revelation principle. Under expected utility, signals that recommend the same action can be merged without changing incentives. Under CVaR, such a merge may change the active tail event and therefore change the receiver's ranking of actions. Thus the appropriate reduced form is not indexed by actions alone, but by actions together with their active CVaR facets.

For each action  $a \in \mathcal{A}$ , let  $\mathcal{L}_a$  be the finite index set from Lemma 1, so that

$$f_a(\mu) = \text{CVaR}_r^\mu(u(\cdot, a)) = \max_{\ell \in \mathcal{L}_a} \langle c_{a,\ell}, \mu \rangle.$$

For every pair  $(a, \ell)$ , define the refined incentive region

$$P_{a,\ell} := \{ \mu \in \Delta(\Omega) : \langle c_{a,\ell}, \mu \rangle \geq \langle c_{a',\ell'}, \mu \rangle \text{ for all } a' \in \mathcal{A}, \ell' \in \mathcal{L}_{a'} \}. \quad (8)$$

If  $\mu \in P_{a,\ell}$ , then facet  $\ell$  is active for action  $a$ , and action  $a$  is a weak best response for the receiver. Since all comparisons are linear, each  $P_{a,\ell}$  is a polytope.

This yields a refined revelation principle. Although signals cannot in general be merged by action alone, they can be grouped by the pair consisting of the recommended action and an active CVaR facet.

**Proposition 1** (Active-Facet Revelation Principle). *For every incentive-compatible signaling scheme in the finite-state CVaR persuasion problem, there exists another incentive-compatible signaling scheme with the same sender value whose signals are indexed by pairs  $(a, \ell)$ , where  $a \in \mathcal{A}$  is the recommended action and  $\ell \in \mathcal{L}_a$  is an active CVaR facet at the induced posterior. Moreover, the posterior associated with signal  $(a, \ell)$  belongs to  $P_{a,\ell}$ .*

Proof in Appendix H.

The resulting problem is linear in the joint distribution over states and refined recommendations.

**Theorem 1** (Exact LP for finite-state CVaR persuasion). *Consider a finite-state Bayesian persuasion problem with a single CVaR receiver, finite action set  $\mathcal{A}$ , explicitly given sender and receiver payoffs, prior  $\mu_0$ , and rational risk level  $r \in (0, 1)$ . Let  $m = |\Omega|$ ,  $n = |\mathcal{A}|$ , and*

$$L := \sum_{a \in \mathcal{A}} |\mathcal{L}_a|.$$

*Then an optimal incentive-compatible signaling scheme can be computed by a linear program with  $mL$  nonnegative joint-mass variables and at most  $m + L^2$  linear constraints, apart from nonnegativity. Since  $L \leq nm$ , this is  $O(nm^2)$  variables and  $O(n^2m^2)$  incentive constraints. In particular, the problem is solvable in time polynomial in  $n$ ,  $m$ , and the input bit length.*

Proof in Appendix I.

The theorem clarifies the role of Lemma 1. CVaR does break the classical action-only revelation argument, because the active tail facet may change under merging. But once the active facet is kept as part of the recommendation type, the incentive regions become polytopes and the sender's optimization problem becomes an ordinary linear program.

The appendices contain two complementary views of this tractability result. Appendix D.1 works out the binary state-action case explicitly, where the geometry of CVaR incentives can be visualized directly. Appendix K gives a fixed-dimensional cell-enumeration argument. Both are subsumed by the active-facet LP in Theorem 1, but they help explain why the correct refinement is by action-facet pairs rather than by actions alone.

## 4 The Polyhedral Boundary: Explicit Tractability and Succinct Hardness

The active-facet LP reveals that the tractability of finite-state CVaR persuasion is not specific to the variational formula of CVaR. The essential property is max-affinity: once the receiver's value is represented as the maximum of affine functions of the posterior, each signal can be refined by the affine piece supporting the recommended action. This section makes the corresponding representation boundary precise. If the affine pieces are explicitly listed, the same LP argument remains polynomial. If they are given only through a succinct combinatorial description, the hidden facet structure can encode NP-hard search problems.

### 4.1 Explicitly Listed Polyhedral Risk Preferences

We first record the direct extension of the CVaR result to general polyhedral risk preferences with listed facets.

**Definition 2** (Explicit polyhedral risk preference). *A risk preference is explicit polyhedral if, for every receiver action  $a \in \mathcal{A}$ ,*

$$\rho(\mu, a) = \max_{\ell \in \mathcal{L}_a} \langle c_{a,\ell}, \mu \rangle,$$

*where the finite index set  $\mathcal{L}_a$  and all coefficient vectors  $c_{a,\ell} \in \mathbb{R}^{|\Omega|}$  are given as part of the input. Let  $L := \sum_{a \in \mathcal{A}} |\mathcal{L}_a|$  denote the total number of listed affine pieces.*

CVaR is the leading example of this class. By Lemma 1, each action has at most  $|\Omega|$  affine pieces, and these pieces can be constructed from the payoff table. The next theorem states the general form of the active-facet LP. Its running time is polynomial in the number of states, actions, and listed affine pieces.

**Theorem 2** (Exact LP for explicit polyhedral risk persuasion). *Consider a finite-state Bayesian persuasion problem with finite action set  $\mathcal{A}$ , prior  $\mu_0$ , sender payoff  $v$ , and an explicit polyhedral receiver risk preference as in Definition 2. Let  $m = |\Omega|$  and  $L = \sum_{a \in \mathcal{A}} |\mathcal{L}_a|$ . Then an optimal incentive-compatible signaling scheme can be computed by a linear program with  $mL$  nonnegative joint-mass variables and at most  $m + L^2$  linear constraints, apart from nonnegativity. Hence the problem is solvable in time polynomial in  $m$ ,  $L$ , and the input bit length.*

Proof in Appendix J.

This theorem is a representation statement. Polyhedrality alone is not a source of computational hardness: if all facets are listed, they can be treated as refined recommendation types. Any hardness result must therefore rely on a different representation model, in which the relevant affine pieces are hidden, implicit, or exponentially many.

## 4.2 Succinct Polyhedral Risk and Computational Hardness

We next consider such a representation model. A succinct polyhedral risk preference still has a max-affine form, but the affine pieces are specified by a compact combinatorial rule rather than by an explicit list. Expanding all facets would recover the LP above, but the expanded formulation may have exponential size. Moreover, identifying a useful hidden facet can itself be a hard combinatorial problem.

A polyhedral risk functional is given succinctly if, for each action  $a$ ,

$$\rho(\mu, a) = \max_{\ell \in \mathcal{L}_a} \langle c_{a,\ell}, \mu \rangle,$$

but the index family  $\mathcal{L}_a$  is specified by a polynomial-size combinatorial description rather than by enumeration.

In the reduction, the hidden affine pieces are indexed by the  $K$ -cliques of an input graph, while all payoffs and affine coefficients lie in  $[0, 1]$ .

**Theorem 3** (NP-hardness for succinct polyhedral risk). *Deciding whether a signaling scheme can achieve sender value at least a given threshold is NP-hard for succinctly represented polyhedral risk preferences, even with an explicit finite state space, two receiver actions, and a uniform prior.*

Proof in Appendix L.

Together, Theorems 2 and 3 identify a representation boundary. Max-affine risk preferences are tractable when their affine pieces are listed, but the same structure can be computationally hard when those pieces are given only implicitly. The obstruction is therefore not nonlinearity per se, but the representation of the receiver’s polyhedral risk landscape.

## 5 Posterior Discretization for Finite-Statistic Risk Preferences

The hardness result above is an exact worst-case statement for arbitrary succinct descriptions of polyhedral risk. We now turn to a finite-precision setting. The approximation problem does not require recovering every hidden facet of the receiver’s risk landscape; it only requires preserving the posterior statistics that determine the receiver’s evaluation. This leads to approximate incentive compatibility rather than exact incentive compatibility. For implicit statistic families, the relevant input model is the cell-separation model in Assumption 1.

**Assumption 1** (Finite-statistic cell access). *There exist statistic functions*

$$g_1, \dots, g_D : \Omega \rightarrow \mathbb{R}, \quad |g_j(\omega)| \leq C_g,$$

*and maps  $\Psi_a : \mathbb{R}^D \rightarrow \mathbb{R}$ , one for each action  $a \in \mathcal{A}$ , such that*

$$\rho(\mu, a) = \Psi_a(\langle g_1, \mu \rangle, \dots, \langle g_D, \mu \rangle). \quad (9)$$

*Each  $\Psi_a$  is  $L_\Psi$ -Lipschitz in the  $\ell_\infty$ -norm. The algorithm can evaluate  $\rho(\bar{\mu}, a)$  at grid posteriors and can enforce the statistic cells used below: given a grid center  $\bar{\mu}$ , a tolerance  $\eta$ , and a candidate posterior  $\mu$ , it can either certify*

$$\max_{j \in [D]} |\langle g_j, \mu - \bar{\mu} \rangle| \leq \eta \quad (10)$$

*or return a violated statistic. This condition is satisfied when the statistics are explicitly listed; more generally, it may be imposed through a polynomial-time separation oracle for the statistic cells.*

This access condition is used only for the finite-precision scheme; the exact LPs for CVaR and explicitly listed polyhedral risks do not rely on it.

For max-affine risks, the statistics can be chosen as the affine pieces. If

$$\rho(\mu, a) = \max_{\ell \in \mathcal{L}_a} \langle c_{a,\ell}, \mu \rangle,$$

then set  $g_{a,\ell} = c_{a,\ell}$ . In this case  $D = \sum_a |\mathcal{L}_a|$  and  $L_\Psi = 1$ . For CVaR, Lemma 1 gives  $D \leq mn$  and  $C_g \leq M_R(1 + 2/r)$ . For succinct polyhedral risks,  $D$  may be exponentially large. The bounds below depend on  $\log D$ , while the LP implementation relies on the cell-access condition in Assumption 1.

For the discretization bounds, write

$$B_\rho := C_g L_\Psi. \quad (11)$$

**Sampling finite statistics.** The discretization uses the standard empirical approximation argument for finite families of bounded linear statistics. A posterior need not be approximated in every coordinate of the simplex; it is enough to approximate the statistics through which the receiver's risk value changes. The state-contingent LP then enforces these statistic cells directly.

### 5.1 Discretization by $k$ -Uniform Distributions

The belief simplex  $\Delta(\Omega)$  is continuous, so we replace it with the finite grid of  $k$ -uniform distributions. For  $k \in \mathbb{N}$ , let

$$\mathcal{D}_k = \left\{ \mu \in \Delta(\Omega) : \mu(\omega) \in \left\{ 0, \frac{1}{k}, \dots, 1 \right\} \text{ for every } \omega \right\}. \quad (12)$$

Its cardinality is

$$|\mathcal{D}_k| = \binom{m+k-1}{k} \leq m^k.$$

The grid must approximate receiver values for all actions. Under the finite-statistic representation, it is enough to approximate the statistics  $\langle g_j, \mu \rangle$  uniformly.

**Lemma 2** (Uniform finite-statistic approximation by  $k$ -uniform posteriors). *Suppose Assumption 1 holds. For any posterior  $\mu \in \Delta(\Omega)$  and any  $\epsilon_R > 0$ , if  $k \geq \frac{2B_\rho^2}{\epsilon_R^2} \log(2D)$ , then there exists a  $k$ -uniform posterior  $\bar{\mu} \in \mathcal{D}_k$  such that*

$$\max_{j \in [D]} |\langle g_j, \mu - \bar{\mu} \rangle| \leq \frac{\epsilon_R}{L_\Psi}. \quad (13)$$

Consequently,

$$\max_{a \in \mathcal{A}} |\rho(\mu, a) - \rho(\bar{\mu}, a)| \leq \epsilon_R. \quad (14)$$

*Proof.* Sample  $X_1, \dots, X_k$  independently from  $\mu$ , and let  $\bar{\mu}$  be the empirical distribution. For a fixed statistic  $g_j$ , Hoeffding's inequality gives

$$\Pr \left( |\langle g_j, \bar{\mu} - \mu \rangle| \geq \frac{\epsilon_R}{L_\Psi} \right) \leq 2 \exp \left( -\frac{k\epsilon_R^2}{2B_\rho^2} \right).$$

Taking a union bound over the  $D$  statistics, the probability that (13) fails is at most

$$2D \exp \left( -\frac{k\epsilon_R^2}{2B_\rho^2} \right).$$

By the choice of  $k$ , this probability is smaller than one, so there exists an empirical posterior satisfying (13). The Lipschitz condition then implies, for every action  $a$ ,

$$|\rho(\mu, a) - \rho(\bar{\mu}, a)| \leq L_\Psi \max_j |\langle g_j, \mu - \bar{\mu} \rangle| \leq \epsilon_R.$$

□

The preceding lemma shows that every posterior can be represented, for the purpose of receiver incentives, by a nearby grid posterior in terms of the statistics that determine the receiver's risk values. We now encode this approximation as linear cell constraints.

**Definition 3** (Finite-statistic cell). For a grid posterior  $\bar{\mu} \in \mathcal{D}_k$  and tolerance  $\epsilon_R > 0$ , define

$$\mathcal{C}_{\epsilon_R}(\bar{\mu}) = \left\{ \mu \in \Delta(\Omega) : \max_{j \in [D]} |\langle g_j, \mu - \bar{\mu} \rangle| \leq \frac{\epsilon_R}{L_\Psi} \right\}. \quad (15)$$

By Lemma 2, these cells cover the belief simplex. If  $\mu \in \mathcal{C}_{\epsilon_R}(\bar{\mu})$ , then

$$\max_{a \in \mathcal{A}} |\rho(\mu, a) - \rho(\bar{\mu}, a)| \leq \epsilon_R.$$

The cell construction controls how receiver values change when moving from a grid center  $\bar{\mu}$  to any posterior inside its cell. We therefore allow as signal labels all actions that are approximately optimal at the grid center.

**Definition 4** (Approximate-center signal labels). For  $\epsilon_R > 0$ , define

$$\widehat{\Sigma} = \left\{ (\bar{\mu}, a) \in \mathcal{D}_k \times \mathcal{A} : \rho(\bar{\mu}, a) \geq \max_{a' \in \mathcal{A}} \rho(\bar{\mu}, a') - 2\epsilon_R \right\}. \quad (16)$$

The construction of  $\widehat{\Sigma}$  uses only value access at grid posteriors.

## 5.2 The Algorithm and Performance Guarantees

Fix an accuracy parameter  $\epsilon > 0$ , set  $\epsilon_R = \epsilon/4$ , and choose  $k$  as in Lemma 2. The algorithm is as follows.

1. **Grid generation.** Construct  $\mathcal{D}_k$ .
2. **Filtering approximate-center signals.** Construct  $\widehat{\Sigma}$  using Definition 4 and value access to  $\rho(\bar{\mu}, a)$ .
3. **State-contingent optimization.** Solve the LP below over variables  $\varphi(\omega, \sigma)$ , where  $\omega \in \Omega$  and  $\sigma = (\bar{\mu}_\sigma, a_\sigma) \in \widehat{\Sigma}$ .

$$\max_{\varphi} \sum_{\omega \in \Omega} \mu_0(\omega) \sum_{\sigma \in \widehat{\Sigma}} \varphi(\omega, \sigma) v(\omega, a_\sigma) \quad (17a)$$

$$\text{s.t.} \quad \sum_{\sigma \in \widehat{\Sigma}} \varphi(\omega, \sigma) = 1, \quad \forall \omega \in \Omega, \quad (17b)$$

$$\sum_{\omega \in \Omega} \mu_0(\omega) \varphi(\omega, \sigma) \left( g_j(\omega) - \langle g_j, \bar{\mu}_\sigma \rangle + \frac{\epsilon_R}{L_\Psi} \right) \geq 0, \quad \forall \sigma \in \widehat{\Sigma}, \forall j \in [D], \quad (17c)$$

$$\sum_{\omega \in \Omega} \mu_0(\omega) \varphi(\omega, \sigma) \left( g_j(\omega) - \langle g_j, \bar{\mu}_\sigma \rangle - \frac{\epsilon_R}{L_\Psi} \right) \leq 0, \quad \forall \sigma \in \widehat{\Sigma}, \forall j \in [D], \quad (17d)$$

$$\varphi(\omega, \sigma) \geq 0, \quad \forall \omega \in \Omega, \forall \sigma \in \widehat{\Sigma}. \quad (17e)$$

The program is linear in  $\varphi$ . Its cell constraints enforce closeness of the induced posterior to the grid center in all statistics  $g_j$ , rather than in all coordinates of the posterior or in all hidden facets of the risk representation.

**Lemma 3** (Soundness of the State-Contingent LP). Let  $\varphi$  be any feasible solution to LP (17). Then  $\varphi$  induces a valid signaling scheme. Every supported signal  $\sigma \in \widehat{\Sigma}$  satisfies

$$\text{Reg}_{IC}(\mu_\sigma, a_\sigma) \leq 4\epsilon_R,$$

where  $\mu_\sigma$  is the posterior induced by signal  $\sigma$ . In particular, if  $\epsilon_R = \epsilon/4$ , the induced scheme is  $\epsilon$ -IC.

Proof in Appendix M.1.

**Lemma 4** (Completeness of the State-Contingent LP). *Let  $OPT$  denote the optimal sender value among exact-IC signaling schemes. Suppose that there exists an optimal exact-IC signaling scheme with finite support. Then the optimal value of LP (17) is at least  $OPT$ .*

Proof in Appendix M.2.

**Theorem 4** (Finite-Precision Discretization). *Assume the finite-statistic cell-access model of Assumption 1. For any  $\epsilon > 0$ , let*

$$k = O\left(\frac{B_\rho^2 \log D}{\epsilon^2}\right).$$

*Then the discretized state-contingent LP returns a signaling scheme with IC regret at most  $\epsilon$  at every supported posterior-action pair and sender utility at least  $OPT$ . When the statistics are explicitly listed, the running time is*

$$m^{O(B_\rho^2 \log D / \epsilon^2)} \text{poly}(m, n, D, T_{\text{eval}}).$$

*With implicit statistics and statistic-cell separation, the polynomial dependence on  $D$  is replaced by the separation cost.*

When  $B_\rho$  is bounded and  $D$  is polynomial in the explicit input size, the running time is quasi-polynomial in the input size and in  $1/\epsilon$ . The value comparison is against the exact-IC benchmark; because the output is allowed  $\epsilon$ -IC, its sender value may exceed the exact-IC optimum.

Here  $T_{\text{eval}}$  is the cost of evaluating  $\rho(\bar{\mu}, a)$  at a grid posterior, and  $T_{\text{cell}}$  is the cost of separating the statistic-cell constraints. In the explicitly listed case, the LP includes these constraints directly; in the separated case, it is solved by a standard cutting-plane or ellipsoid method.

*Proof.* By Lemma 3, any feasible solution of LP (17) induces a signaling scheme with IC regret at most  $4\epsilon_R = \epsilon$ . By Lemma 4, the LP optimal value is at least  $OPT$ . Therefore the LP optimizer induces a signaling scheme with sender value at least  $OPT$  and IC regret at most  $\epsilon$ .

It remains to bound the running time. Since

$$|\mathcal{D}_k| = \binom{m+k-1}{k} \leq m^k,$$

we have

$$|\widehat{\Sigma}| \leq n|\mathcal{D}_k| \leq nm^k.$$

If the statistics are explicitly listed, the LP has  $m|\widehat{\Sigma}|$  variables and  $O(m|\widehat{\Sigma}| + D|\widehat{\Sigma}|)$  constraints. More generally, if the statistics are implicit, the cell constraints are handled through the cell-separation oracle in Assumption 1; a standard cutting-plane or ellipsoid method then solves the separated LP in time polynomial in the represented size and the oracle costs. Substituting

$$k = O\left(\frac{B_\rho^2 \log D}{\epsilon^2}\right)$$

gives the claimed bound. □

### 5.3 From Approximate IC to Strict IC via Margin Filtering

Theorem 4 gives a scheme whose recommended actions have uniformly bounded IC regret. This approximate guarantee is unavoidable near receiver indifference boundaries: if two actions have nearly equal receiver risk value at a posterior, an  $O(\epsilon)$  perturbation of that posterior can change the exact best response. We next record a standard margin condition under which the same discretization yields signal-wise strict incentive compatibility.

**Definition 5** (IC Margin and Margin-Filtered Signal Labels). *For a posterior-action pair  $(\mu, a)$ , define the IC margin*

$$\Gamma(\mu, a) := \rho(\mu, a) - \max_{a' \neq a} \rho(\mu, a'). \quad (18)$$

*For  $\gamma > 0$ , define the margin-filtered signal alphabet*

$$\widehat{\Sigma}_\gamma = \left\{ (\bar{\mu}, a) \in \mathcal{D}_k \times \mathcal{A} : \Gamma(\bar{\mu}, a) \geq \frac{\gamma}{2} \right\}. \quad (19)$$

**Proposition 2** (Margin Stability under Risk-Value Approximation). *If  $\bar{\mu}$  is an  $\epsilon$ -proxy of  $\mu$  in the sense that*

$$\max_{a \in \mathcal{A}} |\rho(\mu, a) - \rho(\bar{\mu}, a)| \leq \epsilon, \quad (20)$$

*then, for every action  $a$ ,*

$$\Gamma(\bar{\mu}, a) \geq \Gamma(\mu, a) - 2\epsilon. \quad (21)$$

Proof in Appendix M.3.

Strict IC is a stability property rather than a purely optimality property. Exact IC permits ties in the receiver's best-response correspondence, and such ties can be reversed by arbitrarily small posterior perturbations. We therefore state the strict-IC guarantee relative to a margin-restricted benchmark. Let  $OPT_\gamma$  denote the optimal sender value among signaling schemes whose every supported recommendation has IC margin at least  $\gamma$ . The positive margin keeps the benchmark away from the IC boundary and allows the discretized scheme to preserve strict incentives.

**Theorem 5** (Strict IC under a Margin Condition). *Suppose there exists a finite-support benchmark scheme with sender value  $OPT_\gamma$  whose every supported posterior-action pair has IC margin at least  $\gamma > 0$ . Run the finite-precision scheme with the margin-filtered alphabet  $\widehat{\Sigma}_\gamma$  and choose  $\epsilon_R < \gamma/4$ . Then the induced signaling scheme is strictly incentive compatible and has sender value at least  $OPT_\gamma$ .*

*With  $\epsilon_R = \gamma/8$ , the running time is*

$$m^{O(B_\rho^2 \log D / \gamma^2)} \text{poly}(m, n, D, T_{\text{eval}}, T_{\text{cell}})$$

*in the explicitly listed-statistic case, with the analogous separated-oracle bound when statistic-cell constraints are separated.*

Indeed, every supported signal satisfies  $\Gamma(\mu_\sigma, a_\sigma) \geq \frac{\gamma}{2} - 2\epsilon_R > 0$ . For CVaR,  $D \leq mn$  and  $B_\rho = C_R = M_R(1 + 2/r)$ , giving  $m^{O(C_R^2 \log(mn) / \gamma^2)} \text{poly}(m, n)$ . For fixed  $r$  and normalized payoffs, this is quasi-polynomial.

Proof in Appendix M.4.

## 5.4 A Local Active-Facet Refinement

The finite-statistic discretization in Theorem 4 is a global certificate: it controls every statistic that may affect the receiver's value. For max-affine risks, including CVaR and explicitly listed polyhedral risks, these statistics can be taken to be the affine pieces. The resulting global certificate is conservative when the relevant posteriors lie in a small region of the simplex. In that case, many affine pieces can never be active and need not enter the local certificate.

Fix a posterior region  $\mathcal{U} \subseteq \Delta(\Omega)$  and a radius  $\eta > 0$ , and let

$$\mathcal{U}^\eta := \{\nu \in \Delta(\Omega) : \text{dist}_1(\nu, \mathcal{U}) \leq \eta\}.$$

For a max-affine risk

$$\rho(\mu, a) = \max_{\ell \in \mathcal{L}_a} \langle c_{a,\ell}, \mu \rangle,$$

define the local active-facet family

$$\mathcal{F}_{\text{loc}} := \{(a, \ell) : \exists \nu \in \mathcal{U}^\eta \text{ such that } \rho(\nu, a) = \langle c_{a,\ell}, \nu \rangle\}, \quad N_{\text{loc}} := |\mathcal{F}_{\text{loc}}|.$$

Thus  $N_{\text{loc}}$  is the number of affine pieces that can matter near the posteriors under consideration.

The local refinement replaces the global statistic family by  $\mathcal{F}_{\text{loc}}$ . Its proof follows the same soundness-completeness argument as Theorem 4, with the global uniform approximation event replaced by a local one over  $\mathcal{F}_{\text{loc}}$ .

**Theorem 6** (Local Discretization Bound). *Suppose a benchmark scheme is supported on  $\mathcal{U}$ , and suppose the reduced state-contingent LP uses grid centers in  $\mathcal{D}_k \cap \mathcal{U}^\eta$  and is certified to induce only posteriors in  $\mathcal{U}^\eta$ . Then the global max-affine family in Theorem 4 can be replaced by the local family  $\mathcal{F}_{\text{loc}}$ , while preserving the same value and IC-regret guarantees.*

In particular, if

$$V_{\text{loc}} := \sup_{\mu \in \mathcal{U}} \max_{(a, \ell) \in \mathcal{F}_{\text{loc}}} \text{Var}_{\omega \sim \mu} [c_{a, \ell}(\omega)],$$

then it suffices to take

$$k_{\text{loc}} = \tilde{O} \left( \max \left\{ \frac{V_{\text{loc}}}{\epsilon^2}, \frac{C_R}{\epsilon} \right\} \log N_{\text{loc}} \right),$$

where  $C_R$  bounds the affine coefficients. The resulting grid size is at most  $m^{k_{\text{loc}}}$ .

Proof in Appendix N.

The theorem is a refinement, not a replacement, for the global discretization scheme. The global scheme gives a certificate over the whole simplex; the local version explains why an instance can be easier when all relevant posteriors remain in a region with few active facets. A cutting-plane implementation can start with  $\mathcal{F}_{\text{loc}}$ , solve the reduced LP, check the full IC violation, and add any violated facets until the desired certificate is reached.

## 6 Conclusion

This paper studies Bayesian persuasion when the receiver evaluates actions by CVaR rather than expected utility. The change in preferences alters the standard reduced form: action-based recommendations are no longer stable under merging, because the receiver’s tail-risk ranking may change at the merged posterior.

The main conclusion is that this failure is structural, not computationally fatal. In the explicit finite-state model, CVaR has a finite max-affine representation. Refining signals by the active affine piece restores linear incentive constraints and yields an exact active-facet LP. The same reasoning extends to any explicitly listed polyhedral risk preference. Hardness appears only after changing the representation model: when the affine pieces are given succinctly, hidden facets can encode combinatorial search.

The finite-precision results complement this boundary. They are not needed to solve the tabular CVaR problem, but they give approximate-IC guarantees when the relevant risk values are determined by finitely many stable posterior statistics. Under a margin condition, the approximate guarantee becomes strict; under local active-facet structure, the discretization cost depends on the number of locally relevant facets rather than the global facet count.

## References

- Carlo Acerbi and Dirk Tasche. On the coherence of expected shortfall. *Journal of Banking & Finance*, 26(7):1487–1503, July 2002.
- Ingo Althöfer. On sparse approximations to randomized strategies and convex combinations. *Linear Algebra and its Applications*, 199:339–355, March 1994.
- Jerry Anunrojwong, Krishnamurthy Iyer, and David Lingenbrink. Persuading risk-conscious agents: A geometric approach. *Operations Research*, 72(1):151–166, January 2024.
- Itai Arieli and Yakov Babichenko. Private bayesian persuasion. *Journal of Economic Theory*, 182: 185–217, 2019.
- Philippe Artzner, Freddy Delbaen, Jean-Marc Eber, and David Heath. Coherent measures of risk. *Mathematical Finance*, 9(3):203–228, July 1999.
- Yakov Babichenko and Siddharth Barman. Computational aspects of private Bayesian persuasion. In *8th innovations in theoretical computer science conference (ITCS)*, 2017.
- Yakov Babichenko, Inbal Talgam-Cohen, and Konstantin Zabarnyi. Bayesian Persuasion under Ex Ante and Ex Post Constraints. *Proceedings of the AAAI Conference on Artificial Intelligence*, 35(6):5127–5134, May 2021.
- Yakov Babichenko, Inbal Talgam-Cohen, Haifeng Xu, and Konstantin Zabarnyi. Regret-minimizing Bayesian persuasion. *Games and Economic Behavior*, 136:226–248, November 2022.

- Ashwinkumar Badanidiyuru, Kshipra Bhawalkar, and Haifeng Xu. Targeting and signaling in ad auctions. In *Proceedings of the 2018 Annual ACM-SIAM Symposium on Discrete Algorithms*, pages 2545–2563, January 2018.
- Dirk Bergemann and Stephen Morris. Information design: A unified perspective. *Journal of Economic Literature*, 57(1):44–95, March 2019.
- Umang Bhaskar, Yu Cheng, Young Kun Ko, and Chaitanya Swamy. Hardness results for signaling in Bayesian zero-sum and network routing games. In *Proceedings of the 17th ACM Conference on Economics and Computation*, EC '16, pages 479–496, July 2016. ISBN 978-1-4503-3936-0.
- Matteo Castiglioni, Andrea Celli, Alberto Marchesi, and Nicola Gatti. Online bayesian persuasion. In *Advances in neural information processing systems (NeurIPS)*, volume 33, pages 16188–16198, 2020.
- Laura Doval and Vasiliki Skreta. Constrained information design. *Mathematics of Operations Research*, 49(1):78–106, 2024.
- Shaddin Dughmi. On the hardness of signaling. In *IEEE 55th annual symposium on foundations of computer science (FOCS)*, pages 354–363, 2014.
- Shaddin Dughmi and Haifeng Xu. Algorithmic Bayesian persuasion. *SIAM Journal on Computing*, 50(3):16–68, January 2021. Num Pages: STOC16-97.
- Piotr Dworzak and Alessandro Pavan. Preparing for the worst but hoping for the best: Robust (Bayesian) persuasion. *Econometrica*, 90(5):2017–2051, 2022. \_eprint: <https://onlinelibrary.wiley.com/doi/pdf/10.3982/ECTA19107>.
- Yiding Feng, Chien-Ju Ho, and Wei Tang. Rationality-robust information design: Bayesian persuasion under quantal response. In *Proceedings of the 2024 Annual ACM-SIAM Symposium on Discrete Algorithms*, pages 501–546, January 2024.
- C. Filippi, G. Guastaroba, and M.G. Speranza. Conditional value-at-risk beyond finance: A survey. *International Transactions in Operational Research*, 27(3):1277–1319, May 2020.
- Lance Fortnow, Russell Impagliazzo, Valentine Kabanets, and Christopher Umans. On the complexity of succinct zero-sum games. *Computational Complexity*, 17:353–376, 2008. doi: 10.1007/s00037-008-0252-2.
- Hana Galperin and Avi Wigderson. Succinct representations of graphs. *Information and Control*, 56(3):183–198, 1983. doi: 10.1016/S0019-9958(83)80004-7.
- J. Gan, R. Majumdar, G. Radanovic, and A. Singla. Bayesian persuasion in sequential decision-making. In *Proceedings of the AAAI Conference on Artificial Intelligence*, volume 36, pages 4806–4813, 2022.
- Ju Hu and Xi Weng. Robust persuasion of a privately informed receiver. *Economic Theory*, 72(3): 909–953, October 2021.
- Philippe Jorion. *Value at risk, 3rd ed.: The new benchmark for managing financial risk*. McGraw Hill Professional, November 2006. ISBN 978-0-07-173692-3. Google-Books-ID: nnblKhI7KP8C.
- Emir Kamenica and Matthew Gentzkow. Bayesian persuasion. *American Economic Review*, 101(6): 2590–2615, October 2011.
- Svetlana Kosterina. Persuasion with unknown beliefs. *Theoretical Economics*, 17(3):1045–1073, 2022.
- Richard J. Lipton, Evangelos Markakis, and Aranyak Mehta. Playing large games using simple strategies. In *Proceedings of the 4th ACM conference on Electronic commerce*, EC '03, pages 36–41, New York, NY, USA, June 2003. ISBN 978-1-58113-679-1.
- Christos H. Papadimitriou and Mihalis Yannakakis. A note on succinct representations of graphs. *Information and Control*, 71(3):181–185, 1986. doi: 10.1016/S0019-9958(86)80009-2.

- Zinovi Rabinovich, Albert Xin Jiang, Manish Jain, and Haifeng Xu. Information disclosure as a means to security. In *Proceedings of the 2015 International Conference on Autonomous Agents and Multiagent Systems, AAMAS '15*, pages 645–653, Richland, SC, May 2015. ISBN 978-1-4503-3413-6.
- R. Tyrrell Rockafellar and Stanislav Uryasev. Optimization of conditional value-at-risk. *The Journal of Risk*, 2(3):21–41, 2000.
- R. Tyrrell Rockafellar and Stanislav Uryasev. Conditional value-at-risk for general loss distributions. *Journal of Banking & Finance*, 26(7):1443–1471, July 2002.
- Aviad Rubinstein. Honest signaling in zero-sum games is hard, and liars get paid. In *IEEE 58th annual symposium on foundations of computer science (FOCS)*, pages 345–356, 2017.
- Klaus W. Wagner. The complexity of combinatorial problems with succinct input representation. *Acta Informatica*, 23:325–356, 1986. doi: 10.1007/BF00289117.
- Haifeng Xu. On the tractability of public persuasion with no externalities. In *Proceedings of the 31st Annual ACM-SIAM Symposium on Discrete Algorithms*, pages 2708–2727, 2020.
- Haifeng Xu, Zinovi Rabinovich, Shaddin Dughmi, and Milind Tambe. Exploring information asymmetry in two-stage security games. In *Proceedings of the AAAI Conference on Artificial Intelligence*, pages 1057–1063, Austin, Texas, January 2015. ISBN 978-0-262-51129-2.
- Kunhe Yang and Hanrui Zhang. Computational aspects of bayesian persuasion under approximate best response. *arXiv preprint arXiv:2402.07426*, 2024.
- Rong Yang, Christopher Kiekintveld, Fernando Ordóñez, Milind Tambe, and Richard John. Improving resource allocation strategies against human adversaries in security games: An extended study. *Artificial Intelligence*, 195:440–469, February 2013.

## A Limitations and Broader Impacts

**Limitations.** The results are developed for finite state and action spaces with a known prior, known sender and receiver utilities, and a fixed CVaR risk level. These assumptions isolate the effect of nonlinear risk preferences, but they abstract away from learning, misspecification, dynamic feedback, and uncertainty about the receiver’s risk attitude. The exact LP relies on explicit enumeration of states, actions, and CVaR facets; it may become impractical or unavailable in very large, oracle-described, or combinatorial environments. The discretization results address finite-precision implementation and suggest tools for such extensions, but they do not by themselves solve all large-scale variants. The numerical experiments, if included, should be viewed as synthetic illustrations of the theory rather than empirical evidence for deployed systems.

**Broader impacts.** The paper is theoretical, but its motivation is tied to information design in risk-sensitive decision systems. A positive use of the framework is to evaluate whether a disclosure policy remains persuasive when receivers care about tail losses, such as rare failures in medical triage, security alerts, financial advice, or automated platform governance. By making tail risk explicit, the model can help identify when average-case persuasion is misleading and when stronger disclosure is needed for robust decisions. At the same time, persuasion tools can be misused: a sender with accurate knowledge of receiver risk preferences may design information to steer behavior while hiding unfavorable tail events or exploiting near-indifference boundaries. The results should therefore be interpreted as analytical tools for auditing and designing risk-aware information policies, not as an endorsement of manipulative deployment. The work does not release models, datasets, or decision systems, and the experiments, if included, use only synthetic instances.

## B Extended Related Work

**Bayesian persuasion and algorithmic information design.** Bayesian persuasion was introduced by Kamenica and Gentzkow [2011]. In the standard model, the receiver maximizes expected utility,

so each action value is linear in the posterior. This linearity underlies the concavification approach and the reduction to direct recommendations. Subsequent work has developed broad extensions of information design; see Bergemann and Morris [2019] for a survey. On the computational side, optimal signaling admits linear programming formulations in several expected-utility settings [Xu et al., 2015, Dughmi and Xu, 2021], while hardness appears in models with additional strategic or representational complexity, including multiple receivers and related public-signaling variants [Dughmi, 2014, Bhaskar et al., 2016, Rubinstein, 2017, Babichenko and Barman, 2017, Arieli and Babichenko, 2019, Xu, 2020]. Our work differs from these results in the source of nonlinearity: the receiver remains a single decision maker, but her preference over actions is nonlinear in the posterior.

**Risk-conscious persuasion.** Risk-sensitive preferences have been studied in economics, operations research, and finance through coherent risk measures and CVaR [Artzner et al., 1999, Rockafellar and Uryasev, 2000, 2002, Acerbi and Tasche, 2002, Jorion, 2006, Filippi et al., 2020]. In information design, the closest conceptual predecessor is Anunrojwong et al. [2024], who study risk-conscious receivers and identify geometric differences from expected-utility persuasion. Our contribution is computational and structural. We show that CVaR breaks the action-based revelation principle, but that its finite max-affine structure restores tractability through an active-facet refinement. The same observation extends to explicitly listed polyhedral risk preferences.

**Representation and hardness.** The distinction between explicit and succinct representations is central to our complexity results. This distinction is classical in computational complexity: succinct graph representations can turn otherwise simple or standard graph properties into substantially harder decision problems [Galperin and Wigderson, 1983, Papadimitriou and Yannakakis, 1986], and related phenomena appear broadly in combinatorial problems with succinct input descriptions [Wagner, 1986]. Similar representation effects also arise in succinctly represented games, where payoff tables are given implicitly rather than in normal form [Fortnow et al., 2008].

Our hardness result should be read in this representation-theoretic sense. When all affine pieces of a polyhedral risk preference are listed, the active-facet LP is polynomial in the listed input size. When the same family of affine pieces is represented implicitly by a compact combinatorial description, the hidden facets can encode NP-hard search. Thus the result is not a hardness statement for tabular CVaR persuasion, but a representation-boundary result for polyhedral risk landscapes.

**Approximation by sampling and discretization.** The finite-precision scheme uses a sampling argument in the spirit of sparse approximations for games. Althöfer [1994] show that small-support mixed strategies can approximate payoffs against large action sets, and Lipton et al. [2003] apply this idea to approximate Nash equilibria. Related sampling ideas also appear in algorithmic persuasion and robust Stackelberg models [Gan et al., 2022, Yang and Zhang, 2024]. Our use is different: the sampled posterior approximates a finite family of statistics that determine the receiver’s risk value. This gives an approximate-IC finite-precision certificate rather than an exact solution of the succinct polyhedral problem.

**Robustness and bounded rationality.** A separate literature studies robust persuasion under uncertainty about the receiver’s prior, information, or utility function [Hu and Weng, 2021, Kosterina, 2022, Dworzak and Pavan, 2022, Castiglioni et al., 2020, Babichenko et al., 2022]. Other work replaces exact best responses with behavioral or approximate response models [Yang and Zhang, 2024, Feng et al., 2024]. These models are related in spirit because they weaken the classical expected-utility benchmark, but their technical structure is different. Here the receiver is fully optimizing; the difficulty comes from the nonlinear risk functional used to evaluate actions.

## C Mixed-Integer Linear Programming Formulation

This appendix is included only for comparison with the earlier cell-selection view; it is not used in any result.

The cardinality bound and the piecewise-linear representation of CVaR give a direct mixed-integer linear formulation of the Sender’s problem.

We index the signals by  $i \in \mathcal{I} = \{1, \dots, |\Omega|\}$ . We introduce the following decision variables:

- $x_{i,a,\omega} \in [0, 1]$ : The joint probability that the state is  $\omega$ , signal  $i$  is generated, and action  $a$  is recommended.
- $y_{i,a} \in \{0, 1\}$ : An indicator variable equal to 1 if signal  $i$  recommends action  $a$ , and 0 otherwise.
- $\delta_{i,a,l} \in \{0, 1\}$ : An indicator variable equal to 1 if the  $l$ -th linear hyperplane defines the CVaR value for action  $a$  under signal  $i$ .

The optimization model is formulated as follows:

$$\max_{x,y,\delta} \sum_{i \in \mathcal{I}} \sum_{a \in \mathcal{A}} \sum_{\omega \in \Omega} v(\omega, a) x_{i,a,\omega} \quad (22a)$$

$$\text{s.t.} \quad \sum_{i \in \mathcal{I}} \sum_{a \in \mathcal{A}} x_{i,a,\omega} = \mu_0(\omega), \quad \forall \omega \in \Omega \quad (22b)$$

$$\sum_{\omega \in \Omega} x_{i,a,\omega} \leq y_{i,a}, \quad \forall i \in \mathcal{I}, a \in \mathcal{A} \quad (22c)$$

$$\sum_{a \in \mathcal{A}} y_{i,a} = 1, \quad \forall i \in \mathcal{I} \quad (22d)$$

$$\sum_{l \in \mathcal{L}_a} \delta_{i,a,l} = y_{i,a}, \quad \forall i \in \mathcal{I}, a \in \mathcal{A} \quad (22e)$$

$$\sum_{\omega \in \Omega} c_{a,l}(\omega) x_{i,a,\omega} \geq \sum_{\omega \in \Omega} c_{a',j}(\omega) x_{i,a,\omega} - M(1 - \delta_{i,a,l})$$

$$\forall i \in \mathcal{I}, \forall a \in \mathcal{A}, \quad \forall l \in \mathcal{L}_a, \forall a' \in \mathcal{A} \setminus \{a\}, \forall j \in \mathcal{L}_{a'} \quad (22f)$$

Constraint (22b) enforces Bayes-plausibility. Constraints (22c)-(22e) establish logical relationships: each signal recommends exactly one action, and for the recommended action, exactly one linear hyperplane is identified as the active CVaR constraint.

Constraint (22f) represents the non-convex Incentive Compatibility (IC) conditions using the *Big-M* method. It guarantees that if action  $a$  is recommended under signal  $i$  and its CVaR is evaluated on hyperplane  $l$  (i.e.,  $\delta_{i,a,l} = 1$ ), this value must be greater than or equal to the CVaR of any alternative action  $a'$  evaluated on any of its hyperplanes  $j$ . The constant  $M$  is chosen to be sufficiently large ( $M \geq \max_{\omega,a} u(\omega, a) - \min_{\omega,a} u(\omega, a)$ ) to relax the constraint when  $\delta_{i,a,l} = 0$ .

When the state space dimension  $|\Omega|$  is fixed, the number of binary variables in this MILP scales polynomially with  $n$ . This formulation gives an alternative cell-selection view of the geometry. It is not needed for computation in the explicit finite-state CVaR model, since Theorem 1 gives a polynomial-size LP without binary variables. We include it only to relate the active-facet formulation to the earlier cell-enumeration perspective.

## D Geometric Insights and Fixed-Dimension Tractability

### D.1 Geometric Insights from Low-Dimensional Cases

This appendix is not needed for the general tractability result in Theorem 1. It serves as a geometric illustration of the active-facet refinement in the smallest nontrivial case.

To understand how risk consciousness alters the persuasion landscape, consider a binary state space  $\Omega = \{\omega_0, \omega_1\}$  and a binary action space  $\mathcal{A} = \{a_0, a_1\}$ . The Receiver's belief is characterized by a scalar  $\mu = \Pr(\omega_1) \in [0, 1]$ .

#### D.1.1 Convexity of Incentive-Compatible Sets

In the standard risk-neutral model, the linearity of expected utility ensures that the set of beliefs supporting a specific action is convex. Under CVaR preferences, although the utility  $\rho(\mu, a)$  is non-linear, we find that it retains critical structural properties in low dimensions.

**Proposition 3.** *In the  $2 \times 2$  setting with CVaR preferences, the incentive-compatible belief set  $I(a) = \{\mu \in [0, 1] \mid \rho(\mu, a) \geq \rho(\mu, a')\}$  is a convex set (i.e., a closed interval).*

*Proof Sketch.* The CVaR function is the pointwise supremum of linear functions, making it convex. In 1D, the "dominance region" defined by the intersection of two convex piecewise linear functions (with specific monotonicity rooted in the binary state structure) remains a connected interval. (See Appendix F.1 for the detailed proof).

Proposition 3 assures us that the belief space is not fragmented into disjoint islands of optimality. Given this convexity, the Sender's induced utility function  $\hat{v}(\mu)$  retains a piecewise constant structure over connected intervals. This allows us to extend the classical geometric solution method to the risk-conscious setting.

**Proposition 4** (Geometry of Optimization). *In the binary CVaR framework, the solution structure of the Bayesian Persuasion problem is geometrically consistent with the standard expected utility case. Specifically, the Sender's optimal signaling scheme can be effectively solved via the method of **Concavification** of the Sender's value function over the belief space.*

Proposition 4 (proven in Appendix F.2) confirms that the "greedy" structure of optimal persuasion holds: the optimal scheme involves at most two signals inducing beliefs at the boundaries of the incentive-compatible intervals. Since the solution form remains a threshold-based strategy, the impact of risk aversion is entirely captured by the *location* of this threshold. We now quantify this shift using the concept of risk premium.

The deviation of the CVaR threshold  $\mu^{CVaR}$  from the risk-neutral threshold  $\mu^{EU}$  is driven by the *CVaR Risk Premium*,  $P_a(\mu) = \mathbb{E}_\mu[u(\cdot, a)] - \rho(\mu, a)$ . If the risky action  $a_1$  carries a higher risk premium than the safe action  $a_0$ , the Receiver requires a strictly higher posterior probability of the "good" state to accept  $a_1$ . This quantifies how risk aversion shifts the persuasion threshold and reduces the range of beliefs under which the risky action can be induced.

**Proposition 5** (Threshold Shifts and Risk Premium). *Let  $\mu^{CVaR}$  and  $\mu^{EU}$  denote the indifference thresholds for the CVaR and standard models, respectively. Let  $P_a(\mu) = \mathbb{E}_\mu[u(a)] - \rho(\mu, a)$  be the risk premium.*

- **Case 1 (High-Belief Action):** *If  $I(a_1) = [\mu^*, 1]$ , then  $\mu^{CVaR} > \mu^{EU}$  if and only if  $P_{a_1}(\mu^{EU}) > P_{a_0}(\mu^{EU})$ .*
- **Case 2 (Low-Belief Action):** *If  $I(a_1) = [0, \mu^*]$ , then  $\mu^{CVaR} < \mu^{EU}$  if and only if  $P_{a_1}(\mu^{EU}) > P_{a_0}(\mu^{EU})$ .*
- **Case 3:** *If risk premiums are equal,  $\mu^{CVaR} = \mu^{EU}$ .*

## D.2 An Alternative View of Tractability in Bounded State Spaces

The active-facet LP in Theorem 1 gives a polynomial algorithm even when  $m = |\Omega|$  is part of the input. The fixed-dimensional argument below is therefore included only as an alternative geometric view: it enumerates the cells induced by CVaR affine pieces and recovers tractability when  $m$  is fixed.

**Theorem 7** (Polynomial Time for Fixed  $|\Omega|$ ). *If the state space size  $|\Omega| = m$  is a fixed constant, the optimal signaling scheme can be computed in time polynomial in the number of actions  $n$ .*

*Proof Idea.* The core insight relies on the geometry of the Receiver's decision landscape. The Receiver's preference between any two actions is determined by the sign of the difference of their CVaR utilities (Lemma 1). Since CVaR is a piecewise linear convex function (defined by at most  $m$  linear segments per action), the condition  $\rho(\mu, a) \geq \rho(\mu, a')$  can be decomposed into a finite set of linear inequalities.

Consider the collection of all linear hyperplanes that define the boundaries between the utility segments of all actions. The total number of such hyperplanes scales linearly with  $n$ . In a fixed  $m$ -dimensional space, an arrangement of  $N$  hyperplanes partitions the simplex into at most  $O(N^m)$  convex regions (cells). Inside each cell, the Receiver's "best response" is invariant (or the problem reduces to a simple linear comparison).

Consequently, finding the optimal signaling scheme reduces to selecting a set of at most  $m$  cells from this partition and determining the optimal weights and locations within them to decompose the prior  $\mu_0$ . Since the number of cells is polynomial in  $n$ , we can efficiently enumerate the candidate support sets. The rigorous construction of this hyperplane arrangement and the counting argument are provided in Appendix K.  $\square$

## E A Finite-Support Bound for General Risk Preferences

This appendix recalls a standard support-reduction argument for finite-state persuasion. The result is a variant of the splitting lemma in Bayesian persuasion [Kamenica and Gentzkow, 2011]; related finite-support and Carathéodory-type reductions appear in Babichenko et al. [2021] and Doval and Skreta [2024]. We include the statement only as a background geometric fact.

**Lemma 5** (Finite posterior support). *For any Bayesian persuasion problem with a finite state space  $\Omega$  and an arbitrary receiver risk functional  $\rho(\mu, a)$ , there exists an optimal signaling scheme supported on at most  $|\Omega|$  posterior beliefs, provided an optimal Bayes-plausible distribution over posteriors exists.*

*Proof.* Let  $m = |\Omega|$ . A signaling scheme can be represented by a Bayes-plausible distribution  $\tau$  over posterior beliefs:

$$\int_{\Delta(\Omega)} \mu d\tau(\mu) = \mu_0.$$

For each posterior  $\mu$ , let

$$W(\mu) := \max_{a \in \arg \max_{a'} \rho(\mu, a')} \sum_{\omega \in \Omega} \mu(\omega) v(\omega, a)$$

be the sender's payoff at  $\mu$ , with sender-favorable tie-breaking. The sender's objective is

$$\int_{\Delta(\Omega)} W(\mu) d\tau(\mu).$$

Take an optimal Bayes-plausible distribution  $\tau^*$ . Consider the probability measure on  $\Delta(\Omega) \times \mathbb{R}$  induced by  $\mu \mapsto (\mu, W(\mu))$ . Its expectation is

$$\left( \mu_0, \int W(\mu) d\tau^*(\mu) \right).$$

This point lies in the convex hull of the set

$$\{(\mu, W(\mu)) : \mu \in \Delta(\Omega)\} \subseteq \mathbb{R}^{m+1}.$$

By Carathéodory's theorem, it can be represented as a convex combination of at most  $m + 2$  such points. A standard strengthening for Bayes-plausible persuasion, sometimes called the splitting lemma or the Fenchel–Carathéodory support reduction, removes the objective coordinate and yields an optimal Bayes-plausible distribution supported on at most  $m$  posterior beliefs. Equivalently, there exists an optimal signaling scheme using at most  $|\Omega|$  signals.

The statement is independent of the particular form of  $\rho$ . It is a support-size result only: it does not identify the posterior beliefs or give a tractable description of the receiver's incentive regions.  $\square$

## F Detailed Proofs for Low-Dimensional Case

### F.1 Proof of Proposition 3

We provide a rigorous four-step proof covering convexity, piecewise linearity, continuity, and the convexity of the incentive-compatible set.

**1. Convexity of the Risk Preference** Using the dual representation of CVaR [Rockafellar and Uryasev, 2000], for a utility maximizing agent, the risk preference is defined as:

$$\rho(\mu, a) = \max_{b \in \mathbb{R}} \left( b - \frac{1}{r} \mathbb{E}_\mu[(b - u(\omega, a))^+] \right) \quad (23)$$

Let  $h(b, \mu) = b - \frac{1}{r} [(1 - \mu)(b - u_0)^+ + \mu(b - u_1)^+]$ , where  $\mu = \Pr(\omega_1)$ . For any fixed  $b$ ,  $h(b, \mu)$  is a linear function of  $\mu$ . Since  $\rho(\mu, a)$  is the pointwise maximum of a family of linear functions (indexed by  $b$ ), it is inherently a convex function of  $\mu$ .

**2. Explicit Piecewise Linear Representation** Without loss of generality, assume the Receiver chooses action  $a_0$  with utilities  $u_{00} = u(\omega_0, a_0)$  and  $u_{10} = u(\omega_1, a_0)$ . Case A: If  $u_{00} < u_{10}$  (utility increases with state), the CVaR takes the form:

$$\rho(\mu, a_0) = \begin{cases} u_{00}, & \text{if } \mu < 1 - r \\ \frac{1}{r}[(1 - \mu)u_{00} + (\mu - (1 - r))u_{10}], & \text{if } \mu \geq 1 - r \end{cases} \quad (24)$$

Case B: If  $u_{00} > u_{10}$  (utility decreases with state), the form is:

$$\rho(\mu, a_0) = \begin{cases} u_{10}, & \text{if } \mu \geq r \\ \frac{1}{r}[\mu u_{10} + (r - \mu)u_{00}], & \text{if } \mu < r \end{cases} \quad (25)$$

In both cases, the function is composed of two linear segments joined at a kink point ( $1 - r$  or  $r$ ). Thus,  $\rho(\mu, a)$  is piecewise linear.

**3. Continuity Verification** We verify continuity at the kink  $\mu^* = 1 - r$  for Case A. The left limit is  $\lim_{\mu \rightarrow (1-r)^-} \rho(\mu, a_0) = u_{00}$ . The value at the kink is:

$$\rho(1 - r, a_0) = \frac{1}{r}[(1 - (1 - r))u_{00} + 0] = \frac{ru_{00}}{r} = u_{00}. \quad (26)$$

Since the limit equals the function value,  $\rho(\mu, a_0)$  is continuous. The same logic applies to Case B.

**4. Convexity of the Incentive-Compatible Set.** The Receiver's best-response region for action  $a_k$  is

$$I(a_k) = \{\mu \in [0, 1] : \rho(\mu, a_k) \geq \rho(\mu, a_j)\}.$$

It remains to show that this set is an interval. Write

$$\Delta_a := u(\omega_1, a) - u(\omega_0, a).$$

From the explicit representation above, if  $\Delta_a \geq 0$ , then  $\rho(\mu, a)$  is constant on  $[0, 1 - r]$  and affine on  $[1 - r, 1]$  with slope  $\Delta_a/r$ . If  $\Delta_a < 0$ , then  $\rho(\mu, a)$  is affine on  $[0, r]$  with slope  $\Delta_a/r$  and constant on  $[r, 1]$ .

Consider

$$D(\mu) = \rho(\mu, a_k) - \rho(\mu, a_j).$$

If  $\Delta_{a_k}$  and  $\Delta_{a_j}$  have the same sign, then the two CVaR functions have the same kink point, either  $1 - r$  or  $r$ . Hence  $D(\mu)$  is constant on one side of the kink and affine on the other side. Therefore its superlevel set  $\{\mu : D(\mu) \geq 0\}$  is a closed interval, possibly empty or equal to all of  $[0, 1]$ .

If  $\Delta_{a_k}$  and  $\Delta_{a_j}$  have opposite signs, then one CVaR function is nondecreasing and the other is nonincreasing. Consequently,  $D(\mu)$  is monotone on  $[0, 1]$ ; it is nondecreasing when  $\Delta_{a_k} \geq 0 \geq \Delta_{a_j}$  and nonincreasing in the reverse case. Thus the superlevel set  $\{\mu : D(\mu) \geq 0\}$  is again a closed interval.

In all cases,  $I(a_k) = \{\mu : D(\mu) \geq 0\}$  is a closed interval of  $[0, 1]$ , and therefore it is convex.  $\square$

## F.2 Proof of Proposition 4 (Concavification and LP Formulation)

*Proof.* From Proposition 3, the belief space is partitioned into intervals where the Receiver's action  $a^*(\mu)$  is constant. The Sender's induced utility is  $v(\mu) = \mathbb{E}_\mu[u^S(\omega, a^*(\mu))]$ . Let  $\mu^{CVaR}$  be the threshold separating  $I(a_0)$  and  $I(a_1)$ . Assuming  $a_1$  is induced for  $\mu \geq \mu^{CVaR}$ ,  $v(\mu)$  is a step-like function:

$$v(\mu) = \begin{cases} \mathbb{E}_\mu[u^S(\omega, a_0)] & \text{if } \mu < \mu^{CVaR} \\ \mathbb{E}_\mu[u^S(\omega, a_1)] & \text{if } \mu \geq \mu^{CVaR} \end{cases} \quad (27)$$

The optimal value is given by the concave closure  $V(\mu) = \text{cav}(v)(\mu)$ .

Calculating this concave closure is equivalent to solving the following Linear Program (LP) to find the supporting line  $L(\mu) = k\mu + b$  at  $\mu_0$ :

$$\min_{k, b} \quad k \cdot \mu_0 + b \quad (28a)$$

$$\text{s.t.} \quad k \cdot 0 + b \geq v(0) \quad (28b)$$

$$k \cdot \mu^{CVaR} + b \geq \lim_{\mu \rightarrow (\mu^{CVaR})^-} v(\mu) \quad (28c)$$

$$k \cdot \mu^{CVaR} + b \geq v(\mu^{CVaR}) \quad (28d)$$

$$k \cdot 1 + b \geq v(1) \quad (28e)$$

The constraints ensure the line dominates  $v(\mu)$  at all critical points (boundaries and the discontinuity). The optimal value  $k^*\mu_0 + b^*$  corresponds to the Sender's maximum expected utility. If  $V(\mu_0) > v(\mu_0)$ , the optimal signal induces the beliefs corresponding to the binding constraints (typically 0 and  $\mu^{CVaR}$ ).  $\square$

### F.3 Proof of Proposition 5 (Threshold Shifts)

*Proof.* We analyze the shift for **Case 1**, where  $I(a_0) = [0, \mu^*]$  and  $I(a_1) = [\mu^*, 1]$ . The thresholds are defined by the indifference conditions:

$$\text{Risk Neutral: } \mathbb{E}_\mu[u(a_1)] = \mathbb{E}_\mu[u(a_0)] \implies \Delta U(\mu^{EU}) = 0 \quad (29)$$

$$\text{CVaR: } \rho(\mu, a_1) = \rho(\mu, a_0) \quad (30)$$

Using the risk premium definition  $\rho(\mu, a) = \mathbb{E}_\mu[u(a)] - P_a(\mu)$ , the CVaR condition becomes:

$$\mathbb{E}_\mu[u(a_1)] - P_{a_1}(\mu) = \mathbb{E}_\mu[u(a_0)] - P_{a_0}(\mu) \quad (31)$$

Rearranging gives the fundamental equation:

$$\Delta U(\mu) = P_{a_1}(\mu) - P_{a_0}(\mu) \quad (32)$$

In Case 1, since  $a_1$  is preferred for high beliefs,  $\Delta U(\mu)$  is strictly increasing in  $\mu$ . Evaluate the equation at  $\mu = \mu^{EU}$ :

- LHS is  $\Delta U(\mu^{EU}) = 0$ .
- RHS is  $\Delta P(\mu^{EU}) = P_{a_1}(\mu^{EU}) - P_{a_0}(\mu^{EU})$ .

**Subcase 1.1:** If  $P_{a_1}(\mu^{EU}) > P_{a_0}(\mu^{EU})$  (Risky action has higher premium), then RHS  $> 0$ . To satisfy the equality, we must increase the LHS, which requires increasing  $\mu$  (since  $\Delta U$  is increasing). Thus,  $\mu^{CVaR} > \mu^{EU}$ .

**Subcase 1.2:** If  $P_{a_1}(\mu^{EU}) < P_{a_0}(\mu^{EU})$ , then RHS  $< 0$ , implying  $\mu^{CVaR} < \mu^{EU}$ .

For **Case 2** where  $I(a_1) = [0, \mu^*]$  (Action  $a_1$  preferred at low beliefs),  $\Delta U(\mu)$  is decreasing. If  $P_{a_1} > P_{a_0}$ , we still have RHS  $> 0$ . To match this positive value with a decreasing LHS (which is 0 at  $\mu^{EU}$ ), we must *decrease*  $\mu$ . Thus,  $\mu^{CVaR} < \mu^{EU}$ . This covers all cases described in the proposition.  $\square$

## G Proof of Finite-Facet Representation (Lemma 1)

*Proof.* Fix an action  $a \in \mathcal{A}$  and write

$$X_a(\omega) = u(\omega, a). \quad (33)$$

By the reward-side variational representation of CVaR,

$$\rho(\mu, a) = \sup_{b \in \mathbb{R}} \left\{ b - \frac{1}{r} \sum_{\omega \in \Omega} \mu(\omega)(b - X_a(\omega))^+ \right\}. \quad (34)$$

For a fixed posterior  $\mu$ , define

$$F_\mu(b) = b - \frac{1}{r} \sum_{\omega \in \Omega} \mu(\omega)(b - X_a(\omega))^+. \quad (35)$$

Let the distinct values of  $X_a$  be

$$v_1 < v_2 < \dots < v_q, \quad q \leq |\Omega|. \quad (36)$$

The function  $F_\mu(b)$  is concave and piecewise linear in  $b$ , with breakpoints contained in  $\{v_1, \dots, v_q\}$ .

We first show that the supremum over  $b \in \mathbb{R}$  can be restricted to these breakpoints. If  $b < v_1$ , then  $(b - X_a(\omega))^+ = 0$  for all  $\omega$ , so  $F_\mu(b) = b$ , and the maximum over  $(-\infty, v_1]$  is attained at  $v_1$ . If  $b > v_q$ , then  $(b - X_a(\omega))^+ = b - X_a(\omega)$  for all  $\omega$ , so

$$F_\mu(b) = \left(1 - \frac{1}{r}\right) b + \frac{1}{r} \sum_{\omega} \mu(\omega) X_a(\omega). \quad (37)$$

Since  $r \in (0, 1]$ , the coefficient  $1 - 1/r$  is nonpositive, and hence the maximum over  $[v_q, \infty)$  is attained at  $v_q$ .

On each interval  $(v_k, v_{k+1})$ , the set of states satisfying  $X_a(\omega) < b$  is fixed, and therefore  $F_\mu(b)$  is affine in  $b$  on that interval. If an affine function attains its maximum in the interior of an interval, then an endpoint also attains the same maximum. Hence there exists a maximizer among the finite set  $\{v_1, \dots, v_q\}$ . Therefore,

$$\rho(\mu, a) = \max_{k=1, \dots, q} \left\{ v_k - \frac{1}{r} \sum_{\omega \in \Omega} \mu(\omega) (v_k - u(\omega, a))^+ \right\}. \quad (38)$$

For each  $k$ , define the coefficient vector  $c_{a,k} \in \mathbb{R}^{|\Omega|}$  by

$$c_{a,k}(\omega) = v_k - \frac{1}{r} (v_k - u(\omega, a))^+. \quad (39)$$

Since  $\sum_{\omega} \mu(\omega) = 1$ , the  $k$ -th term above can be written as

$$\sum_{\omega \in \Omega} \mu(\omega) c_{a,k}(\omega) = \langle c_{a,k}, \mu \rangle. \quad (40)$$

Thus

$$\rho(\mu, a) = \max_{k=1, \dots, q} \langle c_{a,k}, \mu \rangle, \quad q \leq |\Omega|. \quad (41)$$

Hence  $\rho(\cdot, a)$  is the maximum of finitely many affine functions of  $\mu$ . It is therefore convex, continuous, and piecewise linear on  $\Delta(\Omega)$ .

Finally, if  $|u(\omega, a)| \leq C_R$  for all  $\omega$ , then  $|v_k| \leq C_R$  and  $(v_k - u(\omega, a))^+ \leq 2C_R$ . Therefore

$$|c_{a,k}(\omega)| \leq C_R + \frac{2C_R}{r} = C_R \left( 1 + \frac{2}{r} \right). \quad (42)$$

□

## H Detailed Proofs for Proposition 1

*Proof.* Consider any incentive-compatible signaling scheme. Let  $s$  be a signal with probability  $\lambda_s$ , posterior  $\mu_s$ , and recommended action  $a_s$ . Since  $a_s$  is incentive compatible,

$$f_{a_s}(\mu_s) \geq f_{a'}(\mu_s), \quad \forall a' \in \mathcal{A}.$$

Choose one active facet  $\ell_s \in \mathcal{L}_{a_s}$  such that

$$f_{a_s}(\mu_s) = \langle c_{a_s, \ell_s}, \mu_s \rangle.$$

Then for every  $a' \in \mathcal{A}$  and every  $\ell' \in \mathcal{L}_{a'}$ ,

$$\langle c_{a_s, \ell_s}, \mu_s \rangle = f_{a_s}(\mu_s) \geq f_{a'}(\mu_s) \geq \langle c_{a', \ell'}, \mu_s \rangle.$$

Hence  $\mu_s \in P_{a_s, \ell_s}$ . Relabeling the signal  $s$  by the pair  $(a_s, \ell_s)$  does not change its probability, posterior, recommended action, or sender payoff. Therefore the resulting refined signaling scheme is incentive compatible and has the same sender value.

If several original signals have the same pair  $(a, \ell)$ , they need not be merged at this stage. They can either be kept as separate signals with the same label, or aggregated later in the LP through their joint masses. The key point is that every signal can be assigned to a polyhedral region  $P_{a, \ell}$  determined by an action and an active CVaR facet. □

## I Detailed Proofs for Theorem 1

*Proof.* For each refined recommendation type  $(a, \ell)$ , with  $a \in \mathcal{A}$  and  $\ell \in \mathcal{L}_a$ , and for each state  $\omega \in \Omega$ , introduce a nonnegative variable

$$q_{a, \ell, \omega} \geq 0.$$

It represents the joint probability of state  $\omega$  and a signal that recommends action  $a$  with active CVaR facet  $\ell$ .

The sender's objective is linear:

$$\max_q \sum_{a \in \mathcal{A}} \sum_{\ell \in \mathcal{L}_a} \sum_{\omega \in \Omega} q_{a,\ell,\omega} v(\omega, a).$$

Bayes plausibility requires

$$\sum_{a \in \mathcal{A}} \sum_{\ell \in \mathcal{L}_a} q_{a,\ell,\omega} = \mu_0(\omega), \quad \forall \omega \in \Omega.$$

For incentive compatibility, the posterior induced by a positive-mass refined recommendation  $(a, \ell)$  is

$$\mu_{a,\ell}(\omega) = \frac{q_{a,\ell,\omega}}{\lambda_{a,\ell}}, \quad \lambda_{a,\ell} := \sum_{\omega \in \Omega} q_{a,\ell,\omega}.$$

The condition  $\mu_{a,\ell} \in P_{a,\ell}$  is equivalent, after multiplying by  $\lambda_{a,\ell}$ , to the linear inequalities

$$\sum_{\omega \in \Omega} q_{a,\ell,\omega} (c_{a,\ell,\omega} - c_{a',\ell',\omega}) \geq 0,$$

for every  $a \in \mathcal{A}$ ,  $\ell \in \mathcal{L}_a$ ,  $a' \in \mathcal{A}$ , and  $\ell' \in \mathcal{L}_{a'}$ .

Every feasible solution of the LP induces an incentive-compatible signaling scheme: for each  $(a, \ell)$  with  $\lambda_{a,\ell} > 0$ , send a signal of probability  $\lambda_{a,\ell}$ , posterior  $\mu_{a,\ell}$ , and recommendation  $a$ . The Bayes-plausibility constraints ensure that the posteriors average to the prior, and the linear incentive constraints ensure that  $a$  is a receiver best response at  $\mu_{a,\ell}$ .

Conversely, take any incentive-compatible signaling scheme. For each signal  $s$  recommending action  $a_s$ , choose one active facet  $\ell_s \in \mathcal{L}_{a_s}$  satisfying

$$f_{a_s}(\mu_s) = \langle c_{a_s, \ell_s}, \mu_s \rangle.$$

Since  $a_s$  is incentive compatible,

$$\langle c_{a_s, \ell_s}, \mu_s \rangle = f_{a_s}(\mu_s) \geq f_{a'}(\mu_s) \geq \langle c_{a', \ell'}, \mu_s \rangle$$

for all  $a' \in \mathcal{A}$  and  $\ell' \in \mathcal{L}_{a'}$ . Hence  $\mu_s \in P_{a_s, \ell_s}$ . Assigning joint mass

$$q_{a_s, \ell_s, \omega} \leftarrow q_{a_s, \ell_s, \omega} + \lambda_s \mu_s(\omega)$$

and aggregating signals with the same pair  $(a, \ell)$  gives a feasible LP solution with the same sender value. Therefore the LP optimum equals the optimal persuasion value.

The number of refined types is  $L = \sum_a |\mathcal{L}_a| \leq nm$ , where  $n = |\mathcal{A}|$ . Hence the LP has  $mL \leq nm^2$  nonnegative variables. Bayes plausibility gives  $m$  equalities, and the refined incentive comparisons give at most  $L^2 \leq n^2 m^2$  inequalities. The coefficients are computed from the explicit payoff table and the rational CVaR level  $r$ , so their bit length is polynomial in the input size. Standard polynomial-time linear programming algorithms therefore solve the problem in polynomial time.  $\square$

## J Detailed Proofs for Theorem 2

*Proof.* Let

$$\mathcal{T} := \{(a, \ell) : a \in \mathcal{A}, \ell \in \mathcal{L}_a\}$$

be the set of action–facet recommendation types. For each type  $(a, \ell) \in \mathcal{T}$ , define the polyhedral incentive region

$$P_{a,\ell} := \{\mu \in \Delta(\Omega) : \langle c_{a,\ell}, \mu \rangle \geq \langle c_{a',\ell'}, \mu \rangle \quad \forall (a', \ell') \in \mathcal{T}\}.$$

If  $\mu \in P_{a,\ell}$ , then facet  $\ell$  is active for action  $a$ , and action  $a$  is a weak best response under the risk preference  $\rho$ . Since all inequalities are linear,  $P_{a,\ell}$  is a polytope.

Introduce a nonnegative joint-mass variable

$$q_{a,\ell,\omega} \geq 0, \quad (a, \ell) \in \mathcal{T}, \omega \in \Omega.$$

The intended meaning is the joint probability that the state is  $\omega$  and the sender sends a refined recommendation of type  $(a, \ell)$ . Consider the linear program

$$\begin{aligned} \max_{q \geq 0} \quad & \sum_{(a, \ell) \in \mathcal{T}} \sum_{\omega \in \Omega} q_{a, \ell, \omega} v(\omega, a) \\ \text{s.t.} \quad & \sum_{(a, \ell) \in \mathcal{T}} q_{a, \ell, \omega} = \mu_0(\omega), \quad \forall \omega \in \Omega, \\ & \sum_{\omega \in \Omega} q_{a, \ell, \omega} (c_{a, \ell, \omega} - c_{a', \ell', \omega}) \geq 0, \\ & \forall (a, \ell) \in \mathcal{T}, \forall (a', \ell') \in \mathcal{T}. \end{aligned}$$

The first set of constraints is Bayes plausibility. For a type  $(a, \ell)$  with positive mass

$$\lambda_{a, \ell} := \sum_{\omega \in \Omega} q_{a, \ell, \omega} > 0,$$

the induced posterior is

$$\mu_{a, \ell}(\omega) := \frac{q_{a, \ell, \omega}}{\lambda_{a, \ell}}.$$

The second set of constraints is exactly the homogeneous form of  $\mu_{a, \ell} \in P_{a, \ell}$ . Therefore every feasible solution induces an incentive-compatible signaling scheme: for every positive-mass type  $(a, \ell)$ , send one signal with probability  $\lambda_{a, \ell}$ , posterior  $\mu_{a, \ell}$ , and recommendation  $a$ . The sender value of this scheme is precisely the LP objective.

Conversely, take any incentive-compatible signaling scheme. For each signal  $s$ , let  $\lambda_s$  be its probability,  $\mu_s$  its posterior, and  $a_s$  its recommended action. Since the scheme is incentive compatible,

$$\rho(\mu_s, a_s) \geq \rho(\mu_s, a') \quad \forall a' \in \mathcal{A}.$$

Choose an active facet  $\ell_s \in \mathcal{L}_{a_s}$  such that

$$\rho(\mu_s, a_s) = \langle c_{a_s, \ell_s}, \mu_s \rangle.$$

Then for every  $(a', \ell') \in \mathcal{T}$ ,

$$\langle c_{a_s, \ell_s}, \mu_s \rangle = \rho(\mu_s, a_s) \geq \rho(\mu_s, a') \geq \langle c_{a', \ell'}, \mu_s \rangle.$$

Thus  $\mu_s \in P_{a_s, \ell_s}$ . Adding the joint mass

$$\lambda_s \mu_s(\omega)$$

to the variable  $q_{a_s, \ell_s, \omega}$ , and aggregating over signals with the same action–facet type, gives a feasible LP solution with the same sender value. Hence the LP optimum equals the optimal persuasion value.

The number of variables is  $mL$ . The Bayes-plausibility constraints contribute  $m$  equalities, and the incentive comparisons contribute at most  $L^2$  inequalities. Since all coefficient vectors are explicitly listed, the coefficient bit length is polynomial in the input size. Standard polynomial-time linear programming algorithms therefore solve the problem in time polynomial in  $m, L$ , and the input bit length.  $\square$

## K Detailed Proof of Theorem 7

In this appendix, we provide the rigorous constructive proof for the polynomial-time solvability of the persuasion problem when the state space size  $|\Omega| = m$  is fixed. Write  $n = |\mathcal{A}|$ .

### K.1 Geometric Decomposition of the Belief Simplex

Recall that for each action  $a \in \mathcal{A}$ , the CVaR utility is piecewise linear:

$$\rho(\mu, a) = \max_{l \in \{1, \dots, m\}} \langle \mathbf{c}_{a, l}, \mu \rangle \quad (43)$$

where  $\mathbf{c}_{a, l} \in \mathbb{R}^m$  are constant vectors derived from utility parameters. The Receiver prefers action  $a$  over  $a'$  at belief  $\mu$  if:

$$\max_l \langle \mathbf{c}_{a, l}, \mu \rangle \geq \max_k \langle \mathbf{c}_{a', k}, \mu \rangle \quad (44)$$

This condition holds if there exists an index  $l$  such that for all  $k$ ,  $\langle \mathbf{c}_{a,l}, \mu \rangle \geq \langle \mathbf{c}_{a',k}, \mu \rangle$ . We define the set of **critical hyperplanes**  $\mathcal{H}$  as the set of all loci where any two linear segments (either from the same action or different actions) intersect:

$$\mathcal{H} = \{H_{a,l,a',k} \mid a, a' \in \mathcal{A}; l, k \in \{1, \dots, m\}\} \quad (45)$$

where  $H_{a,l,a',k} = \{\mu \in \mathbb{R}^m \mid \langle \mathbf{c}_{a,l} - \mathbf{c}_{a',k}, \mu \rangle = 0\}$ . The total number of linear segments across all actions is  $N_{seg} \leq mn$ . The number of pairwise comparisons (hyperplanes) is bounded by the square of this number:

$$|\mathcal{H}| \leq (mn)^2 = n^2 m^2 \quad (46)$$

Consider the arrangement  $\mathcal{A}(\mathcal{H})$  formed by these hyperplanes restricted to the  $(m-1)$ -dimensional simplex  $\Delta(\Omega)$ . A classic result in combinatorial geometry states that an arrangement of  $N$  hyperplanes in  $\mathbb{R}^d$  partitions the space into at most  $O(N^d)$  connected regions (cells). Here  $d = m-1$  and  $N = n^2 m^2$ . Thus, the number of cells  $K$  satisfies:

$$K = O((n^2 m^2)^{m-1}) = O(n^{2m-2}) \quad (47)$$

Since  $m$  is a constant,  $K$  is polynomial in  $n$ .

## K.2 Algorithm and Complexity Analysis

Within each open cell  $C$  of the arrangement, the ordering of all linear functions  $\{\langle \mathbf{c}_{a,l}, \mu \rangle\}$  is fixed. This implies: For every action  $a$ , the active linear segment  $l^*(a)$  (where  $\rho(\mu, a)$  attains its maximum) is constant. The Receiver's optimal action set  $A^*(C) = \operatorname{argmax}_a \rho(\mu, a)$  is constant for all  $\mu \in C$ .

### The Algorithm

- **Construct the Arrangement:** Enumerate all  $O(n^{2m})$  cells. This can be done computationally by traversing the graph of the arrangement.
- **Identify Receiver Behavior:** For each cell  $C_j$ , determine the Receiver's best response action  $a_j$ .
- **Optimize Convex Decomposition:** According to Carathéodory's theorem, the optimal signaling scheme requires at most  $m$  posterior beliefs. We iterate over all combinations of  $m$  cells  $\{C_{j_1}, \dots, C_{j_m}\}$  from the arrangement. For each combination, we solve the following Linear Program (LP):

$$\max_{\lambda, \mu_1, \dots, \mu_m} \sum_{k=1}^m \lambda_k v(\mu_k, a_{j_k}) \text{ s.t. } \sum_{k=1}^m \lambda_k \mu_k = \mu_0 \& \mu_k \in \text{closure}(C_{j_k}), \quad \forall k \& \sum \lambda_k = 1, \quad \lambda_k \geq 0$$

(Note: The constraint  $\mu_k \in C_{j_k}$  with variable weight  $\lambda_k$  can be linearized by substituting  $z_k = \lambda_k \mu_k$ , where  $z_k$  must lie in the conic hull of  $C_{j_k}$ ).

The number of cell combinations is  $\binom{K}{m} \approx K^m \approx (n^{2m})^m = n^{2m^2}$ . For each combination, we solve a fixed-size LP. Thus, the total runtime is polynomial in  $n$ , specifically  $O(n^{2m^2})$ .  $\square$

## L Proof of Theorem 3

*Proof.* We reduce from  $K$ -CLIQUE. Let  $G = (V, E)$  be an undirected graph with  $|V| = n$ , and let  $K$  be the target clique size. The persuasion instance has state space

$$\Omega = V,$$

and the prior is uniform:

$$\mu_0(v) = \frac{1}{n}, \quad v \in V.$$

The receiver has two actions, denoted  $a_T$  and  $a_0$ . The sender obtains payoff

$$v(v, a_T) = 1, \quad v(v, a_0) = 0, \quad \forall v \in V.$$

Thus the sender wants to induce action  $a_T$ .

The receiver's risk value for the safe action  $a_0$  is constant:

$$\rho(\mu, a_0) = 1 = \langle \mathbf{1}, \mu \rangle.$$

The receiver's risk value for the target action  $a_T$  is defined by a succinct max-affine representation. Let  $\mathcal{C}_K(G)$  denote the set of all  $K$ -cliques of  $G$ . For every  $C \in \mathcal{C}_K(G)$ , define the affine coefficient vector  $c_C \in \{0, 1\}^V$  by

$$c_C(v) = \mathbf{1}\{v \in C\}.$$

Set

$$\rho(\mu, a_T) = \max_{C \in \mathcal{C}_K(G)} \sum_{v \in C} \mu(v),$$

with the convention that the maximum over an empty family is 0. This is a polyhedral risk functional: it is the maximum of affine functions of the posterior. The family is succinctly represented by the graph  $G$  and the integer  $K$ , rather than by explicitly listing all  $K$ -cliques.

We set the sender-value threshold to

$$\eta = \frac{K}{n}.$$

We now prove that the graph contains a  $K$ -clique if and only if the sender can achieve value at least  $\eta$ .

First suppose that  $G$  contains a  $K$ -clique  $C$ . Consider the signaling scheme that sends signal  $s_T$  exactly on states in  $C$ , and sends signal  $s_0$  otherwise. Conditional on  $s_T$ , the posterior is supported on  $C$ , hence

$$\rho(\mu_{s_T}, a_T) \geq \sum_{v \in C} \mu_{s_T}(v) = 1.$$

Since  $\rho(\mu, a_0) = 1$  for every posterior, action  $a_T$  is a weak best response at  $\mu_{s_T}$ . Conditional on  $s_0$ , recommend  $a_0$ , which is always a weak best response because  $\rho(\mu, a_T) \leq 1 = \rho(\mu, a_0)$ . The probability of signal  $s_T$  is  $K/n$ , so the sender's expected value is

$$\frac{K}{n} \cdot 1 + \left(1 - \frac{K}{n}\right) \cdot 0 = \eta.$$

Thus the persuasion instance has value at least  $\eta$ .

Conversely, suppose that  $G$  has no  $K$ -clique. Then  $\mathcal{C}_K(G) = \emptyset$ , and by construction

$$\rho(\mu, a_T) = 0 \quad \text{for every posterior } \mu.$$

Since  $\rho(\mu, a_0) = 1$ , action  $a_T$  is never incentive compatible at any posterior. Therefore every incentive-compatible signaling scheme recommends  $a_0$  with probability one, and the sender's expected value is  $0 < \eta$ . Hence the sender can achieve value at least  $\eta$  only if  $G$  contains a  $K$ -clique.

The construction is polynomial in the size of  $(G, K)$ . Therefore deciding whether the sender can achieve value at least  $\eta$  is NP-hard.  $\square$

## M Proofs for the Discretization Scheme

Throughout this appendix,  $B_\rho = C_g L_\Psi$  denotes the finite-statistic scale from Section 5. In the CVaR specialization,  $D \leq mn$  and  $B_\rho = C_R = M_R(1 + 2/r)$ , where  $n = |\mathcal{A}|$ . The proofs use the finite-statistic cell-access model of Assumption 1; when the statistics are implicit, the displayed cell constraints are understood through the corresponding separation oracle.

This appendix gives the proofs for Section 5. Appendices M.1 and M.2 prove the LP soundness and completeness lemmas; Appendices M.3 and M.4 prove the strict-IC margin claims. Throughout,  $\bar{\mu}$  denotes the empirical  $k$ -uniform posterior sampled from  $\mu$ .

### M.1 Proof of Lemma 3

*Proof.* Let  $\varphi$  be feasible for LP (17). The constraints (17b) and (17e) define a valid state-contingent signaling rule. For a signal  $\sigma = (\bar{\mu}_\sigma, a_\sigma)$ , let

$$p_\sigma := \sum_{\omega \in \Omega} \mu_0(\omega) \varphi(\omega, \sigma)$$

be its unconditional probability. If  $p_\sigma > 0$ , the induced posterior is

$$\mu_\sigma(\omega) = \frac{\mu_0(\omega)\varphi(\omega, \sigma)}{p_\sigma}.$$

The lower and upper cell constraints imply, after dividing by  $p_\sigma$ , that for every statistic  $j \in [D]$ ,

$$-\frac{\epsilon_R}{L_\Psi} \leq \langle g_j, \mu_\sigma \rangle - \langle g_j, \bar{\mu}_\sigma \rangle \leq \frac{\epsilon_R}{L_\Psi}.$$

By the Lipschitz condition on  $\Psi_a$ , this gives

$$|\rho(\mu_\sigma, a) - \rho(\bar{\mu}_\sigma, a)| \leq \epsilon_R, \quad \forall a \in \mathcal{A}.$$

Since  $\sigma \in \widehat{\Sigma}$ , the recommended action is  $2\epsilon_R$ -optimal at the grid center:

$$\rho(\bar{\mu}_\sigma, a_\sigma) \geq \max_{a' \in \mathcal{A}} \rho(\bar{\mu}_\sigma, a') - 2\epsilon_R.$$

Therefore, for any competing action  $a'$ ,

$$\begin{aligned} \rho(\mu_\sigma, a') &\leq \rho(\bar{\mu}_\sigma, a') + \epsilon_R \\ &\leq \rho(\bar{\mu}_\sigma, a_\sigma) + 3\epsilon_R \\ &\leq \rho(\mu_\sigma, a_\sigma) + 4\epsilon_R. \end{aligned}$$

Thus the IC regret of the recommendation is at most  $4\epsilon_R$ . Signals with zero probability do not affect the induced scheme.  $\square$

## M.2 Proof of Lemma 4

*Proof.* Let  $\pi^*$  be a finite-support exact-IC signaling scheme attaining value  $OPT$ . Index its signals by  $j \in J$ . Let  $p_j$  be the probability of signal  $j$ ,  $\mu_j^*$  its posterior, and  $a_j$  its recommended action. By exact incentive compatibility,

$$\rho(\mu_j^*, a_j) \geq \rho(\mu_j^*, a), \quad \forall a \in \mathcal{A}.$$

For each posterior  $\mu_j^*$ , apply Lemma 2 to choose a  $k$ -uniform posterior  $\bar{\mu}_j \in \mathcal{D}_k$  such that

$$\max_a |\rho(\mu_j^*, a) - \rho(\bar{\mu}_j, a)| \leq \epsilon_R.$$

Then  $(\bar{\mu}_j, a_j) \in \widehat{\Sigma}$ , since for every action  $a$ ,

$$\begin{aligned} \rho(\bar{\mu}_j, a_j) &\geq \rho(\mu_j^*, a_j) - \epsilon_R \\ &\geq \rho(\mu_j^*, a) - \epsilon_R \\ &\geq \rho(\bar{\mu}_j, a) - 2\epsilon_R. \end{aligned}$$

Define a candidate LP solution by aggregating all original signals mapped to the same discretized label:

$$\varphi^*(\omega, \sigma) := \sum_{j: (\bar{\mu}_j, a_j) = \sigma} \pi^*(j | \omega).$$

The signaling-rule and nonnegativity constraints are immediate from the fact that  $\pi^*$  is a signaling scheme.

It remains to verify the cell constraints. Fix  $\sigma = (\bar{\mu}, a_\sigma) \in \widehat{\Sigma}$ , and let

$$J_\sigma = \{j \in J : (\bar{\mu}_j, a_j) = \sigma\}.$$

For every  $j \in J_\sigma$ , Lemma 2 gives

$$|\langle g_l, \mu_j^* - \bar{\mu} \rangle| \leq \frac{\epsilon_R}{L_\Psi}, \quad \forall l \in [D].$$

Multiplying the lower inequality by  $p_j$ , using

$$p_j \mu_j^*(\omega) = \mu_0(\omega) \pi^*(j | \omega),$$

and summing over  $j \in J_\sigma$  yields

$$\sum_{\omega \in \Omega} \mu_0(\omega) \varphi^*(\omega, \sigma) \left( g_l(\omega) - \langle g_l, \bar{\mu} \rangle + \frac{\epsilon_R}{L_\Psi} \right) \geq 0.$$

This is exactly the lower cell constraint. The upper cell constraint follows from the upper inequality in the same way. Hence  $\varphi^*$  is feasible.

Finally, the LP objective at  $\varphi^*$  equals the sender value of the original scheme, because the recommended action attached to each discretized label is the same action used by the original signal mapped to that label:

$$\begin{aligned} & \sum_{\omega \in \Omega} \mu_0(\omega) \sum_{\sigma \in \widehat{\Sigma}} \varphi^*(\omega, \sigma) v(\omega, a_\sigma) \\ &= \sum_{\omega \in \Omega} \mu_0(\omega) \sum_{j \in J} \pi^*(j | \omega) v(\omega, a_j) = OPT. \end{aligned}$$

Thus the LP optimum is at least  $OPT$ .  $\square$

### M.3 Proof of Proposition 2

*Proof.* Fix any competing action  $a' \neq a$ . By the proxy condition,

$$\rho(\bar{\mu}, a) \geq \rho(\mu, a) - \epsilon, \quad \rho(\bar{\mu}, a') \leq \rho(\mu, a') + \epsilon. \quad (48)$$

Therefore

$$\rho(\bar{\mu}, a) - \rho(\bar{\mu}, a') \geq \rho(\mu, a) - \rho(\mu, a') - 2\epsilon. \quad (49)$$

Taking the minimum over  $a' \neq a$  on the left-hand side is equivalent to subtracting the maximum competing value, so

$$\Gamma(\bar{\mu}, a) = \min_{a' \neq a} \{\rho(\bar{\mu}, a) - \rho(\bar{\mu}, a')\} \geq \min_{a' \neq a} \{\rho(\mu, a) - \rho(\mu, a')\} - 2\epsilon = \Gamma(\mu, a) - 2\epsilon. \quad (50)$$

$\square$

### M.4 Proof of Theorem 5

*Proof.* Let  $\pi_{\text{strict}}^* = \{(p_j^*, \mu_j^*, a_j^*)\}_{j \in J}$  be the strict-margin benchmark scheme. By assumption,  $\Gamma(\mu_j^*, a_j^*) \geq \gamma$  for every supported signal  $j$ .

For each  $j$ , apply Lemma 2 to choose  $\bar{\mu}_j \in \mathcal{D}_k$  such that  $\max_{a \in \mathcal{A}} |\rho(\mu_j^*, a) - \rho(\bar{\mu}_j, a)| \leq \epsilon_R$ . By Proposition 2,

$$\Gamma(\bar{\mu}_j, a_j^*) \geq \Gamma(\mu_j^*, a_j^*) - 2\epsilon_R \geq \gamma - 2\epsilon_R. \quad (51)$$

Since  $\epsilon_R \leq \gamma/4$ , we have  $\Gamma(\bar{\mu}_j, a_j^*) \geq \gamma/2$ . Thus  $(\bar{\mu}_j, a_j^*) \in \widehat{\Sigma}_\gamma$ .

Now construct a feasible solution to the margin-filtered LP by the same state-contingent merging argument used in Lemma 4. Because all mapped pairs belong to  $\widehat{\Sigma}_\gamma$ , the construction is feasible for the filtered LP. Since the recommended action  $a_j^*$  is preserved for every original signal, the LP objective value of the constructed solution is exactly  $OPT_{\text{strict}}$ . Therefore the filtered LP optimum is at least  $OPT_{\text{strict}}$ .

It remains to prove strict incentive compatibility of the LP-induced scheme. Let  $\varphi$  be any feasible solution of the filtered LP and consider a supported signal  $\sigma = (\bar{\mu}_\sigma, a_\sigma)$ . Its induced posterior is  $\mu_\sigma$ . The LP cell constraints imply  $\max_{a \in \mathcal{A}} |\rho(\mu_\sigma, a) - \rho(\bar{\mu}_\sigma, a)| \leq \epsilon_R$ . Since  $\sigma \in \widehat{\Sigma}_\gamma$ ,  $\Gamma(\bar{\mu}_\sigma, a_\sigma) \geq \gamma/2$ . Applying Proposition 2 again gives

$$\Gamma(\mu_\sigma, a_\sigma) \geq \Gamma(\bar{\mu}_\sigma, a_\sigma) - 2\epsilon_R \geq \frac{\gamma}{2} - 2\epsilon_R. \quad (52)$$

Because  $\epsilon_R < \gamma/4$ , the right-hand side is strictly positive. Hence  $a_\sigma$  is a strict best response at  $\mu_\sigma$  for every supported signal.

Finally, the running time is the same as in Theorem 4, with  $\epsilon_R = \Theta(\gamma)$ . Hence

$$k = O\left(\frac{B_\rho^2 \log D}{\gamma^2}\right),$$

and the running time is

$$m^{O(B_\rho^2 \log D / \gamma^2)} \text{poly}(m, n, D, T_{\text{eval}}, T_{\text{cell}})$$

in the explicitly listed-statistic case, with the analogous separated-oracle bound under statistic-cell separation.  $\square$

## N Proofs for the Local Active-Facet Refinement

This appendix gives the details for the local refinement in Section 5.4. Throughout this appendix the receiver's risk value is max-affine:

$$\rho(\mu, a) = \max_{\ell \in \mathcal{L}_a} \langle c_{a,\ell}, \mu \rangle.$$

This includes CVaR and, more generally, explicitly listed polyhedral risk preferences. Fix a posterior region  $\mathcal{U} \subseteq \Delta(\Omega)$  and radius  $\eta > 0$ . Let

$$\mathcal{U}^\eta := \{\nu \in \Delta(\Omega) : \text{dist}_1(\nu, \mathcal{U}) \leq \eta\}.$$

The local active-facet family is

$$\mathcal{F}_{\text{loc}} := \{(a, \ell) : \exists \nu \in \mathcal{U}^\eta \text{ such that } \rho(\nu, a) = \langle c_{a,\ell}, \nu \rangle\}, \quad N_{\text{loc}} := |\mathcal{F}_{\text{loc}}|.$$

We also write

$$C_{\text{loc}} := \max_{(a,\ell) \in \mathcal{F}_{\text{loc}}} \|c_{a,\ell}\|_\infty.$$

For CVaR, one may take  $C_{\text{loc}} \leq C_R = M_R(1 + 2/r)$ , where  $M_R = \max_{\omega, a} |u(\omega, a)|$ .

### N.1 A Local Proxy Lemma

The first lemma formalizes why only locally active facets matter. If both posteriors lie in the local neighborhood  $\mathcal{U}^\eta$ , then the value of an action is always realized by a facet in  $\mathcal{F}_{\text{loc}}$ . Hence controlling this smaller family suffices to control all receiver values locally.

**Lemma 6** (Local active-facet proxy). *Let  $\mu \in \mathcal{U}$  and  $\bar{\mu} \in \mathcal{U}^\eta$ . Suppose*

$$\max_{(a,\ell) \in \mathcal{F}_{\text{loc}}} |\langle c_{a,\ell}, \bar{\mu} - \mu \rangle| \leq \epsilon.$$

*Then*

$$\max_{a \in \mathcal{A}} |\rho(\bar{\mu}, a) - \rho(\mu, a)| \leq \epsilon.$$

*Proof.* Fix an action  $a$ . Let  $\ell_{\bar{\mu}} \in \mathcal{L}_a$  be an active facet for action  $a$  at  $\bar{\mu}$ , so that

$$\rho(\bar{\mu}, a) = \langle c_{a,\ell_{\bar{\mu}}}, \bar{\mu} \rangle.$$

Since  $\bar{\mu} \in \mathcal{U}^\eta$ , the pair  $(a, \ell_{\bar{\mu}})$  belongs to  $\mathcal{F}_{\text{loc}}$ . Therefore

$$\begin{aligned} \rho(\bar{\mu}, a) - \rho(\mu, a) &= \langle c_{a,\ell_{\bar{\mu}}}, \bar{\mu} \rangle - \max_{\ell \in \mathcal{L}_a} \langle c_{a,\ell}, \mu \rangle \\ &\leq \langle c_{a,\ell_{\bar{\mu}}}, \bar{\mu} \rangle - \langle c_{a,\ell_{\bar{\mu}}}, \mu \rangle \\ &= \langle c_{a,\ell_{\bar{\mu}}}, \bar{\mu} - \mu \rangle \leq \epsilon. \end{aligned}$$

Conversely, let  $\ell_\mu$  be active for action  $a$  at  $\mu$ . Since  $\mu \in \mathcal{U} \subseteq \mathcal{U}^\eta$ , we have  $(a, \ell_\mu) \in \mathcal{F}_{\text{loc}}$ . Then

$$\begin{aligned} \rho(\mu, a) - \rho(\bar{\mu}, a) &\leq \langle c_{a,\ell_\mu}, \mu \rangle - \langle c_{a,\ell_\mu}, \bar{\mu} \rangle \\ &= \langle c_{a,\ell_\mu}, \mu - \bar{\mu} \rangle \leq \epsilon. \end{aligned}$$

Combining the two inequalities gives  $|\rho(\bar{\mu}, a) - \rho(\mu, a)| \leq \epsilon$ . Taking the maximum over  $a \in \mathcal{A}$  proves the claim.  $\square$

## N.2 Local Uniform Approximation

The next lemma is the local analogue of the global uniform approximation lemma. It uses a union bound only over  $\mathcal{F}_{\text{loc}}$ .

**Lemma 7** (Local concentration over active facets). *Fix  $\mu \in \mathcal{U}$ , and let  $\bar{\mu}$  be the empirical distribution of  $k$  i.i.d. samples from  $\mu$ . With probability at least  $1 - \delta$ ,*

$$\max_{(a,\ell) \in \mathcal{F}_{\text{loc}}} |\langle c_{a,\ell}, \bar{\mu} - \mu \rangle| \leq \epsilon$$

provided

$$k \geq \frac{2C_{\text{loc}}^2}{\epsilon^2} \log \left( \frac{2N_{\text{loc}}}{\delta} \right).$$

Consequently, on the same event, if  $\bar{\mu} \in \mathcal{U}^n$ , then

$$\max_{a \in \mathcal{A}} |\rho(\bar{\mu}, a) - \rho(\mu, a)| \leq \epsilon.$$

*Proof.* Fix  $(a, \ell) \in \mathcal{F}_{\text{loc}}$ . For samples  $X_1, \dots, X_k \sim \mu$ , set  $Y_i = c_{a,\ell}(X_i)$ . Then

$$\frac{1}{k} \sum_{i=1}^k Y_i = \langle c_{a,\ell}, \bar{\mu} \rangle, \quad \mathbb{E}[Y_i] = \langle c_{a,\ell}, \mu \rangle,$$

and  $|Y_i| \leq C_{\text{loc}}$ . Hoeffding's inequality gives

$$\Pr(|\langle c_{a,\ell}, \bar{\mu} - \mu \rangle| > \epsilon) \leq 2 \exp \left( -\frac{k\epsilon^2}{2C_{\text{loc}}^2} \right).$$

Taking a union bound over  $N_{\text{loc}}$  locally active facets yields

$$\Pr \left( \max_{(a,\ell) \in \mathcal{F}_{\text{loc}}} |\langle c_{a,\ell}, \bar{\mu} - \mu \rangle| > \epsilon \right) \leq 2N_{\text{loc}} \exp \left( -\frac{k\epsilon^2}{2C_{\text{loc}}^2} \right).$$

The stated lower bound on  $k$  makes this probability at most  $\delta$ . The final claim follows from Lemma 6.  $\square$

## N.3 A Variance-Sensitive Local Bound

For some instances, the locally active affine pieces have much smaller variance than their worst-case range. The following Bernstein version replaces the range-only sample size by a local variance term.

Define

$$V_{\text{loc}} := \sup_{\mu \in \mathcal{U}} \max_{(a,\ell) \in \mathcal{F}_{\text{loc}}} \text{Var}_{\omega \sim \mu} [c_{a,\ell}(\omega)].$$

**Lemma 8** (Variance-sensitive local active-facet bound). *Fix  $\mu \in \mathcal{U}$ , and let  $\bar{\mu}$  be the empirical distribution of  $k$  i.i.d. samples from  $\mu$ . There is a universal constant  $C > 0$  such that, with probability at least  $1 - \delta$ ,*

$$\max_{(a,\ell) \in \mathcal{F}_{\text{loc}}} |\langle c_{a,\ell}, \bar{\mu} - \mu \rangle| \leq \epsilon$$

provided

$$k \geq C \max \left\{ \frac{V_{\text{loc}}}{\epsilon^2}, \frac{C_{\text{loc}}}{\epsilon} \right\} \log \left( \frac{2N_{\text{loc}}}{\delta} \right).$$

Consequently, if  $\bar{\mu} \in \mathcal{U}^n$ , then  $\max_a |\rho(\bar{\mu}, a) - \rho(\mu, a)| \leq \epsilon$  on the same event.

*Proof.* Fix  $(a, \ell) \in \mathcal{F}_{\text{loc}}$  and again set  $Y_i = c_{a,\ell}(X_i)$ . The random variables are bounded by  $C_{\text{loc}}$ , and their variance is at most  $V_{\text{loc}}$  by definition. Bernstein's inequality gives, for a universal constant  $C_0 > 0$ ,

$$\Pr(|\langle c_{a,\ell}, \bar{\mu} - \mu \rangle| > \epsilon) \leq 2 \exp \left( -C_0 k \min \left\{ \frac{\epsilon^2}{V_{\text{loc}}}, \frac{\epsilon}{C_{\text{loc}}} \right\} \right).$$

A union bound over  $\mathcal{F}_{\text{loc}}$  shows that the desired event holds with probability at least  $1 - \delta$  whenever

$$k \geq C \max \left\{ \frac{V_{\text{loc}}}{\epsilon^2}, \frac{C_{\text{loc}}}{\epsilon} \right\} \log \left( \frac{2N_{\text{loc}}}{\delta} \right)$$

for a sufficiently large universal constant  $C$ . The risk-value conclusion again follows from Lemma 6.  $\square$

## N.4 Proof of the Certified Local Refinement

We now prove the certified local theorem stated in Section 5.4. The statement assumes that the benchmark posteriors lie in  $\mathcal{U}$ , that the reduced LP uses grid centers in  $\mathcal{U}^\eta$ , and that the induced posteriors are certified to remain in  $\mathcal{U}^\eta$ . These conditions ensure that all active facets relevant to the benchmark and to the LP solution belong to  $\mathcal{F}_{\text{loc}}$ .

*Proof of Theorem 6.* The proof is the same soundness-completeness argument as in the global discretization theorem, with the global statistic family replaced by  $\mathcal{F}_{\text{loc}}$ .

*Soundness.* Consider any feasible solution of the reduced state-contingent LP. By assumption, every supported induced posterior  $\mu_\sigma$  lies in  $\mathcal{U}^\eta$ , and its associated grid center  $\bar{\mu}_\sigma$  also lies in  $\mathcal{U}^\eta$ . The local cell constraints guarantee

$$\max_{(a,\ell) \in \mathcal{F}_{\text{loc}}} |\langle c_{a,\ell}, \mu_\sigma - \bar{\mu}_\sigma \rangle| \leq \epsilon_R.$$

By Lemma 6,

$$\max_{a \in \mathcal{A}} |\rho(\mu_\sigma, a) - \rho(\bar{\mu}_\sigma, a)| \leq \epsilon_R.$$

If the signal label  $(\bar{\mu}_\sigma, a_\sigma)$  is chosen from the same approximate-center alphabet as in Theorem 4, then

$$\rho(\bar{\mu}_\sigma, a_\sigma) \geq \max_{a'} \rho(\bar{\mu}_\sigma, a') - 2\epsilon_R.$$

Combining these inequalities gives

$$\max_{a'} \rho(\mu_\sigma, a') - h_0(\mu_\sigma, a_\sigma) \leq 4\epsilon_R.$$

Thus the reduced LP has the same IC-regret soundness guarantee as the global LP.

*Completeness.* Let a benchmark scheme be supported on  $\mathcal{U}$ . For every benchmark posterior  $\mu$ , Lemma 7, or the Bernstein version Lemma 8, gives a grid posterior  $\bar{\mu} \in \mathcal{D}_k$  such that

$$\max_{(a,\ell) \in \mathcal{F}_{\text{loc}}} |\langle c_{a,\ell}, \mu - \bar{\mu} \rangle| \leq \epsilon_R.$$

When the local grid is restricted to  $\mathcal{D}_k \cap \mathcal{U}^\eta$ , we choose such a proxy within  $\mathcal{U}^\eta$ , as required by the theorem's certification condition. Lemma 6 then implies uniform approximation of all receiver values at the benchmark posteriors. Therefore any exact-IC benchmark action becomes an approximate-center label at its local proxy. Assigning the benchmark signal masses to these proxy labels constructs a feasible solution of the reduced LP with the same sender value as the benchmark, exactly as in the completeness proof for the global LP.

The sample-size bound follows from Lemma 8. Taking

$$k_{\text{loc}} = O\left(\max\left\{\frac{V_{\text{loc}}}{\epsilon^2}, \frac{C_{\text{loc}}}{\epsilon}\right\} \log N_{\text{loc}}\right)$$

up to logarithmic confidence factors yields the stated local grid size  $m^{k_{\text{loc}}}$ . The Hoeffding version follows by replacing Lemma 8 with Lemma 7. This proves the theorem.  $\square$

## O Supplementary Numerical Experiments

In this appendix, we provide detailed setups and analyses for the numerical experiments conducted to validate our theoretical findings. We explore three key dimensions: the performance gap between CVaR-aware and risk-neutral persuasion, the impact of risk aversion on information disclosure, and the computational efficiency of our approximation scheme.

### O.1 Implementation Details and Computational Environment

All experiments were implemented in Python. The optimization-based experiments use Gurobi through the `gurobipy` interface. The CVaR-aware persuasion problems are encoded as mixed-integer linear programs: the continuous variables represent the joint probability of state and recommended action, and binary variables select the active linear piece of the CVaR representation. The risk-neutral benchmark in Figure 1 is solved as a linear program with standard expected-utility IC constraints.

Gurobi output was disabled in all reported runs. For the large-instance approximation experiment in Figure 3, the exact benchmark is computed with  $MIPGap=0$ ; approximate runs use  $MIPGap$  equal to the plotted  $\epsilon$  values and a per-solve time limit of 120 seconds. The big- $M$  constant used in the MILP implementation is 10.0.

The deterministic experiments in Figures 1 and 2 do not use random sampling. The discretization scheme experiment in Figure 3 generates synthetic instances with  $|\Omega| = 60$ ,  $n = 20$ ,  $r = 0.25$ , and 20 trials for each  $\epsilon$ . The instance generator supports a NumPy seed argument; in the script used for the reported figure, the trial loop records the intended seed schedule  $42 + t$  for trial  $t$ , but the generator call leaves the seed unset. As a result, rerunning the script reproduces the experimental protocol but may not reproduce the plotted points exactly. A fully deterministic rerun can be obtained by passing the recorded seed  $42 + t$  to the generator in trial  $t$ .

The experiments were run on a MacBook Pro with an Apple M1 Pro processor, 10 CPU cores, and 32GB memory, using macOS 26.4.1. The software environment used Python 3.9.13, NumPy 1.26.4, SciPy 1.13.1, pandas 1.4.4, Matplotlib 3.5.2, and Gurobi/gurobipy 12.0.3. The reported discretization scheme runtime curve records wall-clock time measured around each Gurobi solve; the plotted values aggregate the mean runtime and mean relative error across the 20 trials, with standard-deviation error bars.

## O.2 Performance Comparison: CVaR vs. Risk-Neutral Senders

**Experimental Setup.** We evaluate the Sender’s expected utility under two distinct signaling strategies: our proposed CVaR-aware mechanism versus the standard risk-neutral (expected utility) persuasion model. We vary the Receiver’s risk tolerance level, parameterized by the quantile  $r \in (0, 1)$ , to observe performance robustness.

- **Scenario 1 ( $2 \times 2$  Case):** A minimal setting with two states (Bad/Good) and two actions. The "Safe" action yields a constant utility of 0.4. The "Risky" action yields 0 in the Bad state and 1 in the Good state (Expected Value = 0.5).
- **Scenario 2 ( $5 \times 3$  Case):** A complex setting with 5 states and 3 actions. Action  $a_0$  is safe. Action  $a_1$  is highly risky (20% probability of catastrophic zero return, 80% probability of high return). Action  $a_2$  serves as an intermediate noise option.

### Results and Analysis.

Figure 1 (see main text or placeholder below) illustrates the Sender’s utility as a function of  $r$ .

- **Utility Collapse in Standard Models:** In the  $2 \times 2$  case, the standard risk-neutral model (red dashed line) blindly mixes Good and Bad states to maximize expected value. When  $r$  is low (high risk aversion), this mixed signal fails to satisfy the Receiver’s CVaR constraint, leading the Receiver to reject the risky action entirely. Consequently, the Sender’s utility collapses to 0.
- **Robustness of CVaR Model:** The CVaR-aware model (blue solid line) successfully identifies the Receiver’s "risk floor." At low  $r$ , it adopts a more conservative disclosure strategy to eliminate tail risks, thereby securing a non-zero utility.
- **Convergence:** As  $r \rightarrow 1$ , the Receiver approaches risk neutrality. The CVaR constraints relax, and our model’s performance smoothly converges to the standard benchmark, demonstrating generalized applicability.

## O.3 Impact of Risk Preference on Information Disclosure

**Experimental Setup.** To understand how risk aversion shapes the optimal information structure, we simulate a financial advisory scenario with  $|\Omega| = 5$  states and three actions:

1. **Deposit:** Risk-free, constant utility 0.55.
2. **Bond:** Low risk, linear return profile, expected utility 0.60.
3. **Stock:** High risk, convex return profile (high upside, extreme tail risk of 0), expected utility 0.70.

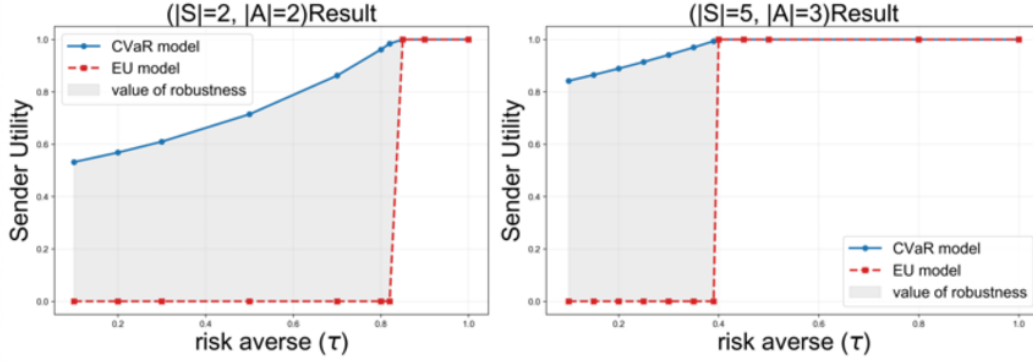


Figure 1: Comparison of Sender's utility under CVaR-aware vs. Standard Expected Utility models across varying risk tolerance levels  $r$ .

The Sender strictly prefers the Receiver to choose "Stock" ( $v_{stock} = 1, v_{others} < 1$ ). We measure the degree of information disclosure using the **posterior entropy**  $H(\pi) = \sum_s \mathbb{P}(s) \mathcal{H}(\mu_s)$ . Lower entropy implies higher disclosure (precision), while higher entropy implies information pooling (ambiguity).

**Results and Analysis.** Figure 2 (placeholder) reveals a monotonic negative correlation between risk tolerance and information precision:

- **High Disclosure at Low  $r$ :** When the Receiver is extremely risk-averse, the Sender is forced to provide high-precision signals to "prove" that the tail risk has been eliminated. Consequently, posterior entropy is low.
- **Strategic Obfuscation at High  $r$ :** As risk tolerance increases, the Sender gains slack to mix "bad" states with "good" ones while still satisfying the CVaR constraint. This allows for partial pooling, leading to higher posterior entropy and higher Sender utility.
- **Step-wise Transitions:** The entropy curve exhibits discrete jumps, corresponding to the Receiver's optimal action switching from Deposit  $\rightarrow$  Bond  $\rightarrow$  Stock as persuasion becomes feasible.

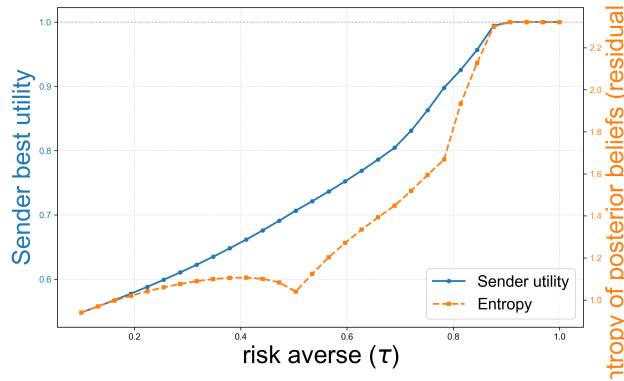


Figure 2: Evolution of posterior entropy (information ambiguity) with respect to risk tolerance  $r$ .

#### O.4 Finite-Precision Discretization: Accuracy-Time Trade-off

We evaluate the discretized implementation as a finite-precision approximation to the active-facet LP. The goal is not to replace the exact LP in the explicit finite-state model, but to illustrate how grid resolution affects sender value and IC violation when posterior beliefs are restricted to a finite representation.

### Experimental Setup.

- **Scale:**  $|\Omega| = 60$  states,  $n = 20$  actions.
- **Adversarial Structure:** To challenge the algorithm, we construct "hard" instances where tail states have double probability weights (simulating frequent crises) and action variances grow exponentially ( $\sigma_a \propto e^{a/3}$ ), creating highly non-convex feasibility boundaries.
- **Parameters:** Risk level  $r = 0.25$ . We vary the approximation parameter  $\epsilon \in \{0.25, \dots, 0.0\}$ .

**Results and Analysis.** Figure 3 (placeholder) plots the Relative Error (Orange) and Running Time (Blue) against  $\epsilon$ .

- **High Precision:** The relative error decreases monotonically with  $\epsilon$ . Notably, at  $\epsilon = 0.05$ , the empirical error is already below 2%, suggesting the algorithm performs much better than the worst-case theoretical bound.
- **Computational Cost:** For coarse approximations ( $\epsilon > 0.08$ ), the runtime is negligible (seconds). However, as  $\epsilon \rightarrow 0$  (specifically  $\epsilon < 0.03$ ), the runtime spikes exponentially. This confirms the theoretical complexity class of  $n^{O(1/\epsilon^2)}$  and highlights the "expensive" nature of exact solutions in this non-convex landscape. The discretization scheme provides a tunable knob to navigate this trade-off effectively.

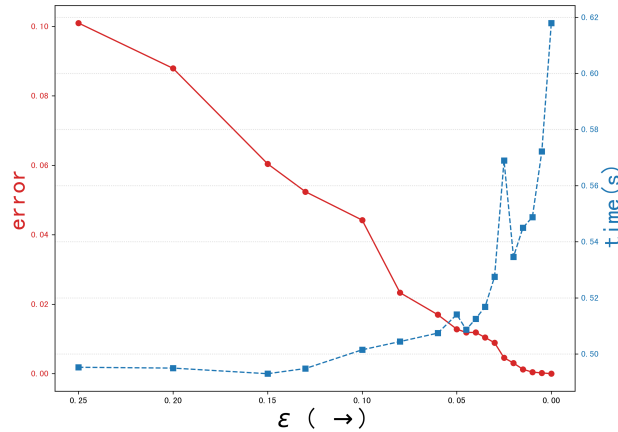


Figure 3: Trade-off between finite-precision accuracy and runtime for the posterior discretization scheme